Improved Measure of Orbital Stability of Rhythmic Motions

by

Amirhosein Khazenifard
B.Eng., Electrical Engineering, Shahed University, Tehran, Iran, 2012
M.A.Sc., Control Systems Engineering, University of Tehran, 2015

A Thesis Submitted in Partial Fulfillment
of the Requirements for the Degree of

MATER OF APPLIED SCIENCE

in the Department of Mechanical Engineering

Supervisory Committee

Improved Measure of Orbital Stability of Rhythmic Motions

by

Amirhosein Khazenifard
B.Eng., Electrical Engineering, Shahed University, Tehran, Iran, 2012
M.A.Sc., Control Systems Engineering, University of Tehran, 2015

Supervisory Committee

Dr. Nikolai Dechev, Department of Mechanical Engineering
Co-Supervisor

Dr. Jooeun Ahn, Department of Mechanical Engineering
Co-Supervisor

Dr. Yang Shi, Department of Mechanical Engineering
Member

Abstract

Supervisory Committee

Dr. Nikolai Dechev, Department of Mechanical Engineering

Co-Supervisor

Dr. Jooeun Ahn, Department of Mechanical Engineering

Co-Supervisor

Dr. Yang Shi, Department of Mechanical Engineering

Member

Rhythmic motion is ubiquitous in nature and technology. Various motions of organisms like the heart beating and walking require stable periodic execution. The stability of the rhythmic execution of human movement can be altered by neurological or orthopedic impairment. In robotics, successful development of legged robots heavily depends on the stability of the controlled limit-cycle. An accurate measure of the stability of rhythmic execution is critical to the diagnosis of several performed tasks like walking in human locomotion. Floquet multipliers have been widely used to assess the stability of a periodic motion. The conventional approach to extract the Floquet multipliers from actual data depends on the least squares method. We devise a new way to measure the Floquet multipliers with reduced bias and estimate orbital stability more accurately. We show that the conventional measure of the orbital stability has bias in the presence of noise, which is inevitable in every experiment and observation. Compared with previous method, the new method substantially reduces the bias, providing acceptable estimate of the orbital stability with fewer cycles even with different noise distributions or higher or lower noise levels. The new method can provide an unbiased estimate of orbital stability within a reasonably small number of cycles. This is important for experiments with human subjects or clinical evaluation of patients that require effective assessment of locomotor stability in planning rehabilitation programs.

Table of Contents

List of Figures

List of Tables

List of Acronyms

Yule-Walker……YW

Least Squares……...LS

Vector Adjusted Ahn Hogan…….....VAAH

Acknowledgments

I am most thankful to Dr. Jooeun Ahn for giving me the chance to pursue my studies in graduate studies at one of the most reputed universities in Canada and world. Many thanks for his technical advice and insight. Also, I would like to thank Dr. Nikolai Dechev for his support through my studies and future career. Finally, I am grateful for the support from Natural Sciences and Engineering Research Council of Canada and Department of Mechanical Engineering at the University of Victoria.

I would like to thank all those who contributed to the development of this study and offer my special thanks to my wife, Ms. Fojan Babaali for her support and patience.

Amirhosein Khazenifard, EIT

Victoria, BC Canada 2017

Dedication

To my lovely wife Fojan and our Family

Chapter 1 - Introduction

1.1 Motivation

There are varieties of rhythmic processes in nature and in various technologies. Accurate measurement of the stability is important in many fields, however performing that measurement is limited in the experiments. One of the examples of this limitation is fluctuations in populations of species which are often periodic (i.e. 17-year cicada) but the number of cycles that may be observed is practically limited [1].

Recent research on legged locomotion in the robotic engineering is progressing from hexapods [2] to bipeds [3, 4] with more focus on walking robots. Also, assessment of the stability is more important than instability as stability is mostly usual due to unpredicted walking environments.

In robotics control systems, the controller design that best stabilizes the cyclic motion can be found by several iterations. Different iterations to find the efficient and effective values of the controller than can stabilize the robotics control systems and kind of trade-off between the amount of energy used for execution of the task. Therefore, an accurate measure of the stability of the rhythmic execution is critical to diagnose the current status; to validate the efficacy of applied control law; and thereby to improve the motor performance more systematically.

Several methods to estimate the stability of rhythmic movements using dynamical systems theories have been explored by others [5, 6, 7, 8].

The main motivation of this research on the stability of rhythmic motions is concerned with neurologically-impaired human subjects while they walk. Their level of functional

recovery needs to be monitored. However, they are usually incapable of walking for extended periods.

In the context of this thesis we analyse how to limit the window of measurement observations and increase the accuracy of the conventional stability measures.

One of the classical examples to assess the stability of rhythmic motions is use of Floquet multipliers. Based on ordinary differential equations theory, Floquet defined the theory for stability of a periodic solution of linear systems. Nowadays many studies in biomechanics, robotics, and ecology still address the rhythmic stability using Floquet theory and the Floquet multiplier [8, 9, 10, 11, 12, 13].

It is important to mention that the original Floquet theory was defined for a deterministic and linear system. However, for the typical systems like robots or eco-systems are involving highly nonlinear dynamics. However, the orbital stability of a limit cycle of a nonlinear system can be addressed by Floquet multiplier of the linearized return map or Poincaré map [14, 15, 16].

Previous studies used a conventional least squares linear fit of the relation between adjacent cycles to assess the orbital stability of rhythmic executions (i.e. human walking) [5, 7, 17, 18, 19, 14]. Hurmuzlu and Basdogan estimated the best affine fit relating the state of each stride with the state of the next one [7]. Dingwell and Kang used a similar approach. According to our studies, none of the prior experimental studies check the validity and the accuracy of the estimation of Floquet multipliers in the presence of noise using the least squares method.

Based on the aforementioned researches on assessment of stability of rhythmic motions using the least squares method, we found out this method in the presence of noise is biased and would not results in an accurate measure of orbital stability. The main motivation and goal of this thesis is to analyze un-biased estimation method to assess the stability of rhythmic executions accurately, and also by reducing the number of cycles required to obtain those.

1.2 Main contributions

The current methods for the accurate assessment of stability of rhythmic motions in experiments with walking models or human walking are questionable. In this thesis we offer the following contributions:

1. Evaluation of the conventional least squares method has shown that the presence of noise has bias. The one-dimensional linearized return map would be studied and new method developed by Ahn and Hogan would be analyzed to reduce the bias of this case [1].
2. A decomposition bias-reduction method for the multi-dimensional linearized return map has developed to solve the problem of biased estimation of Floquet multipliers in high dimensional cases.
3. The application of multi-dimensional methods has been discussed for a walking model as a useful tool, and for the instance of a high dimensional return map.

1.3 Thesis outline

This thesis is structured as follows. Chapter 2 provides the mathematical framework to study the rhythmic executions. It reviews the concept of the return map and defines the one-dimensional and multi-dimensional return map.

Chapters 3 introduce the assessment techniques to measure the orbital stability of rhythmic executions with more focus on rhythmic motions. Both the conventional methods and bias-reduced methods will be discussed in chapter 3 with the details of the simulation results for the one-dimensional and multi-dimensional return maps.

Chapter 4 discusses the estimation methods of chapter 3 and compares the results and discusses the limitations.

Chapter 5 presents the recommendations and directions for future research, and provides the conclusions.

Chapter 2 - Mathematical descriptions of rhythmic motions

2.1 Rhythmic motions systems stability

In theoretical studies of mechanics, the system's stability is defined by how the system's states change in response to perturbations [20]. Also, stability for rhythmic motions that have been considered as periodic motion or limit cycle systems, is defined as "having a constant fixed point that quantifies the tendency of the system's states to return to the periodic limit cycle orbit after the small perturbations". The quantification of this tendency must be between once cycle and the adjacent one and the stability is defined using the Floquet multipliers.

2.2 Return map

The Floquet multipliers are the eigenvalues of the linearization (or Jacobian) of the stride-to-stride function called the Poincaré map or return map. They quantify the stability of periodic cycles by evaluating the local stability of the fixed-point of the Poincaré map.

Floquet theory assumes that the system being studied is periodic, and each state of the system after one period (S_{K+1}) is a function (F) of its current state (S_K) [21];

$$S_{K+1} = F(S_K). \tag{2.1}$$

The function F is determined by the dynamics of system. This discrete map is called the Poincaré map.

The limit cycle, by its definition, becomes a fixed pint (S^*) of the Poincaré map, which satisfies

$$S^* = F(S^*). \tag{2.2}$$

To investigate the local behavior around the limit cycle, we can linearize the map about the fixed point S^*;

$$S_{K+1} - S^* \rightleftharpoons J(S^*)[S_K - S^*] \qquad K = 1,2,\dots,M \quad . \tag{2.3}$$

where J is the Jacobian matrix of the Poincaré map at the fixed point S^*, and M is the total number of cycles which K shows each cycle. Also symbol $\rightleftharpoons$ states approximately equal of left hand side to right hand equation for all of the equations. The eigenvalues of the Jacobian matrix are Floquet multipliers, which determine the local behavior and the stability of the limit cycle. In order to calculate Floquet multipliers from the actual data, it is necessary to reconstruct the time series of the data and estimate the Jacobian matrix.

2.3 One-dimensional return map

In the simplest case of the return map, we address the one-dimensional return map. The linearized return map in a one-dimensional state space that can be expressed as:

$$s_{K+1} - s^* \rightleftharpoons \lambda[s_K - s^*], \qquad K = 1,2,\dots,M \quad . \tag{2.4}$$

Assuming the stochastic noise is added on each cycle as a random variable:

$$s_{K+1} - s^* \rightleftharpoons \lambda[s_K - s^*] + \delta_{k+1}, \quad K = 1,2,\dots,M \quad . \tag{2.5}$$

where δ_{k+1} is from a distribution with zero mean and standard deviation of δ_σ.

Also, the noise in the current cycle is assumed to be independent of the noise in the previous or next cycle. Substituting $s_{K+1} - s^*$ with x_K , the time series will be defined as:

$$x_{K+1} \doteq \lambda x_K + \delta_{k+1} \qquad K = 1,2,\dots,M \quad . \tag{2.6}$$

Where T is the maximum number of stride number, in the Eq. (2.6) and finding the Floquet multiplier consists of estimating the constant λ in the Eq. (2.6).

2.4 Multi-dimensional return map

The typical case of the return map is the multi-dimensional case. Like the Eq. (2.3), the state space representation can be expressed as:

$$S_{K+1} - S^* \doteq J(S^*)[S_K - S^*], \tag{2.7}$$

where J is the Jacobian matrix of the Poincaré map, and assuming stochastic noise added to each cycle:

$$S_{K+1} - S^* = J(S^*)[S_K - S^*] + \Delta_{K+1} \qquad K = 1,2,\dots,M \quad , \tag{2.8}$$

where Δ_{K+1} represents a noise vector from a distribution with zero mean and a covariance matrix of $\Sigma_\Delta = E(\Delta_{K+1}\,\Delta_{K+1}^T)$, where E denotes the expected value [21].

The described equation for the multi-dimensional return map in Eq. (2.8) shows the vector autoregressive (VAR) model of order one.

In order to measure the orbital stability of the rhythmic motion, we need to find the eigenvalues of the Jacobian matrix in Eq. (2.8) and those values are called Floquet multipliers.

2.5 Conclusions

This chapter provided the concept of rhythmic motions as periodic systems. It defined the mathematical model of the Poincaré map as the linearized mapping between each of the cycles. The eigenvalues of the return map assess the orbital stability of the rhythmic motions and define the Floquet multipliers. The one-dimensional linearized return map has been defined simplest case to evaluate the return map with one Floquet multiplier. The multi-dimensional model which contains the VAR model of order one has been introduced to define the concept in the more typical case.

The mathematical framework defined in this chapter can show how to model the rhythmic motion using VAR models of order one. The main challenge, which is discussed in the following chapters, is finding the Floquet multipliers of any VAR model of rhythmic executions to assess the orbital stability of the rhythmic motions. There are different methods to estimate the Floquet multipliers but the main concern is the accuracy of those different methods.

Chapter 3 - Assessment of orbital stability of rhythmic motions

3.1 Conventional methods

As discussed in the chapter 2, the time series of one-dimensional and multi-dimensional cases are autoregressive models, where the standard identification methods for (Auto-Regressive) AR models such as Yule-Walker [22, 23] or Burg [24] could be used to estimate the Floquet multipliers. Least squares method is a special case of Yule-Walker method which has used several times in mentioned researches.

3.1.1 Yule-Walker estimation method

Estimation of the Floquet multipliers using Yule-Walker's method in one or multi-dimensional cases would use the following equations for one and multi-dimensional cases respectively:

$$\hat{\lambda}_{YW} = \frac{\sum_{i=1}^{M-1} x_i x_{i+1}}{\sum_{i=1}^{M-1} x_i^2} \quad , \tag{3.1}$$

$$\hat{J}_{YW} = \frac{\sum_{i=1}^{M-1} X_i X^T{}_{i+1}}{\sum_{i=1}^{M-1} X_i^T X_i} \quad . \tag{3.2}$$

In the Eq. (3.1), x_{K+1} is the substituted form of $s_{K+1} - s^*$ in one-dimensional case and in Eq. (3.1), X_{K+1} is the substituted form of $S_{K+1} - S^*$ as next state representation for the return map. In Eq. (3.2), X_i would be a $K \times 1$ matrix and the resulting $\hat{J}_{YW}$ is $K \times K$ matrix

Yule-Walker's method estimated Floquet multiplier in Eq. (3.1) is $\hat{\lambda}_{YW}$ and the eigenvalues of the estimated Jacobian matrix in Eq. (3.2) are estimated Floquet multipliers.

3.1.2 Burg's method of estimation

Burg used another form of identification as follows. Some of the researched used this equation instead of Yule-Walker's method for AR processes identification [26, 27].

$$\hat{\lambda}_{Burg} = \frac{\sum_{i=1}^{M-1} x_i x_{i+1}}{\frac{x^2(1)}{2} + \sum_{i=2}^{M-1} x_i^2 + \frac{x^2(M)}{2}} \quad , \tag{3.3}$$

$$\hat{J}_{Burg} = \frac{\sum_{i=1}^{M-1} X_i X^T{}_{i+1}}{\frac{X^T X(1)}{2} + \sum_{i=2}^{M-1} X_i X^T{}_{i+1} + \frac{X^T X(M)}{2}} \quad . \tag{3.4}$$

In the Eq. (3.3), $x(1)$ and $x(n)$ are the initial state and final state values of the linearized return map and the main difference based on the equations are those terms in the denominator. In Eq. (3.4), X_i would be a $K \times 1$ matrix and the resulting $\hat{J}_{Burg}$ is $K \times K$ matrix

3.2 Simulation results of conventional methods

In this section, before moving forward to the bias-reduced method, addressing the bias of the previous methods by numerical simulations is necessary. Ahn and Hogan addressed the one-dimensional case using Yule-Walker and Burg's methods [1]. In this thesis, we are using the same method with the generated times series.

With a fixed-values of the Floquet multiplier, λ, the time series of $\{x_K\}$ was constructed by adding the noise. The length of the time series K varied from 10 to 100. Estimation of orbital stability has been addressed using linear regression methods used in previous experimental studies [7, 25].

The simulation and estimation using Yule-Walker and Burg's methods were repeated 1000 times for each K and the bias between the actual λ and the mean of 1000 estimated values, $\hat{\lambda}$ was evaluated for each K.

The test was repeated for three different values of Floquet multiplier, λ, and three types of noise distribution- normal, uniform and asymmetric lognormal.

3.2.1 Yule-Walker's method simulation three different noise distributions

As mentioned in the before section, Yule-Walker's method would be evaluated with three different noise distributions to address the bias of this linear regression method. The time series generated for different cycles for K from 10 to 100 and the estimation repeated 1000 times. The method has been evaluated in one-dimensional case for Floquet multipliers values of 0.2, 0.4 and 0.8.

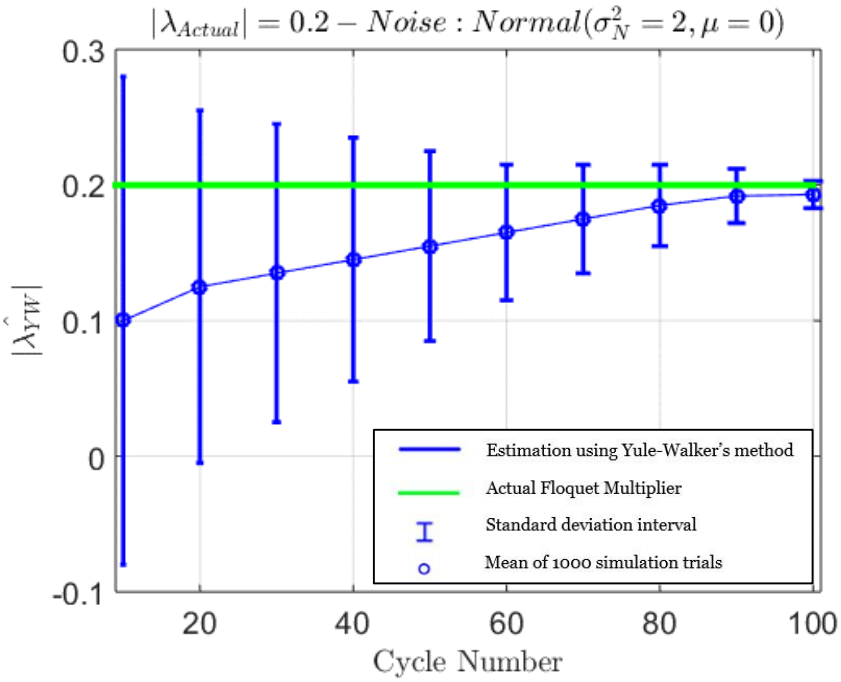

Figure 1. Yule-Walker's method estimation with noise from normal distribution

As shown in Figure 1, there is bias in the estimation using Yule-Walker's method for different cycle numbers for noise, coming from the normal distribution.

The simulations are repeated with another noise distribution, of uniform type, to evaluate the effect of the noise distribution in estimation process.

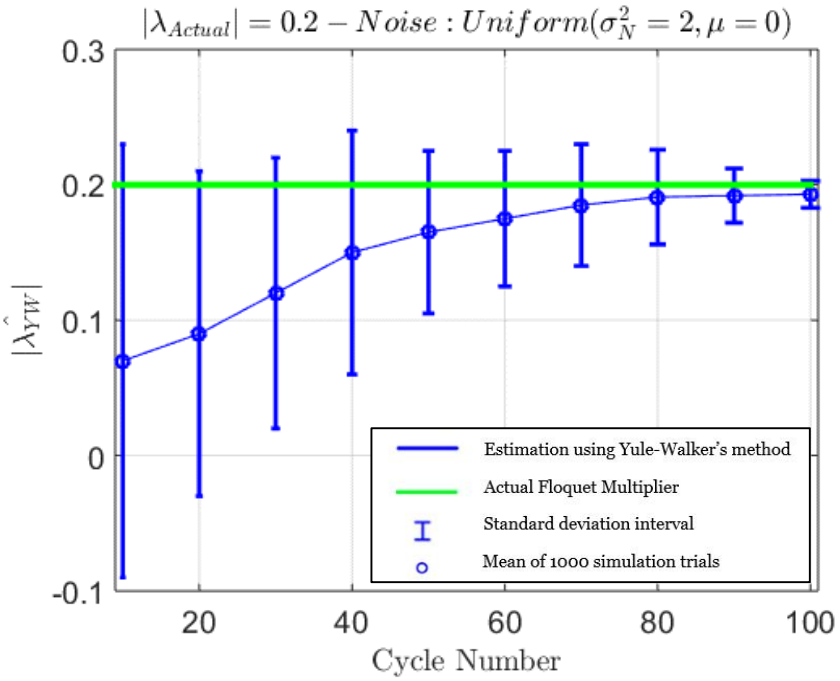

Figure 2. Yule-Walker's method estimation using noise from uniform distribution

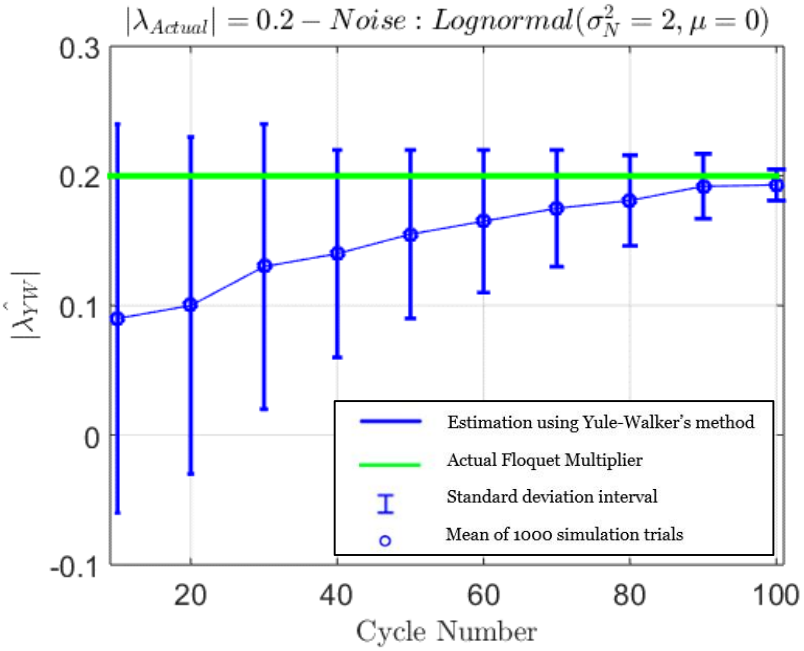

Figure 3. Yule-Walker's method estimation using noise from lognormal distribution

The simulation results of the standard methods for AR processes – Yule-Walker equation yields a substantial bias. Though the accuracy of the estimate improves by increment of cycle number, the convergence is still too slow.

The estimation method using Yule-Walker's equation has been repeated for two different values of the Floquet multipliers 0.4 and 0.8 with normal noise distribution to see the effect of different values on bias.

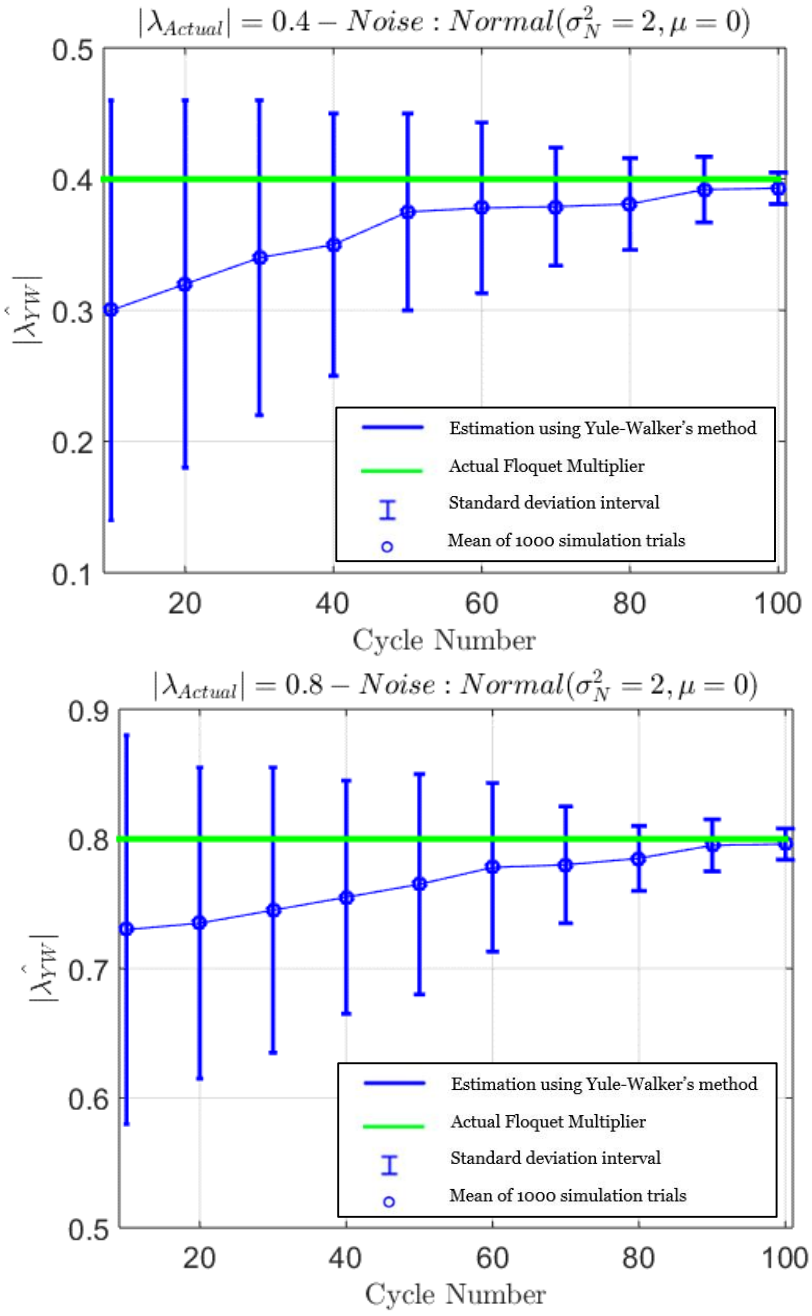

Figure 4. Yule-Walker's method estimation using noise from normal distribution for different values of Floquet multiplier

As shown in Figure 4, the Yule-Walker's method still has bias even with different values of Floquet multipliers. It shows that this method is not accurate enough for the measurement of orbital stability of rhythmic motions until there are enough cycle numbers of 90 or 100. Note that Yule-Walker's method has been widely used in different research to assess local or orbital stability of rhythmic motion like human walking [7, 5].

3.2.2 Burg's method simulation results for three different noise distributions

The conditions for the simulation of Burg's method are the same as Yule-Walker's method. The constructed data has been used but the estimation is based on Eq. (3.2) for the initial and final values of the states in the denominator.

The reason of using Burg's method is to assess the bias of this method in comparison with Yule-Walker's equation. Other research has claimed that this method can resolve some of the limitations of Yule-Walker method [26, 27].

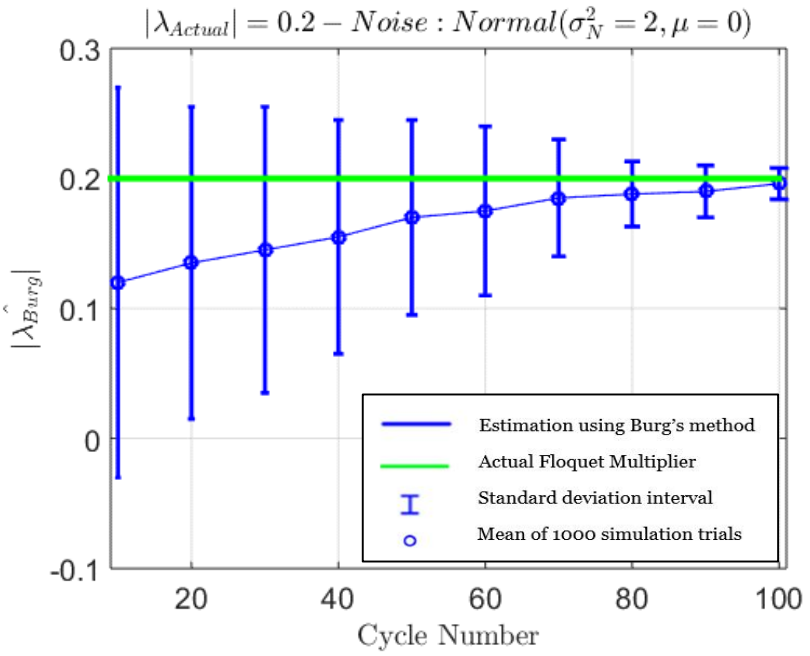

Figure 5. Burg's method estimation using noise from normal distribution

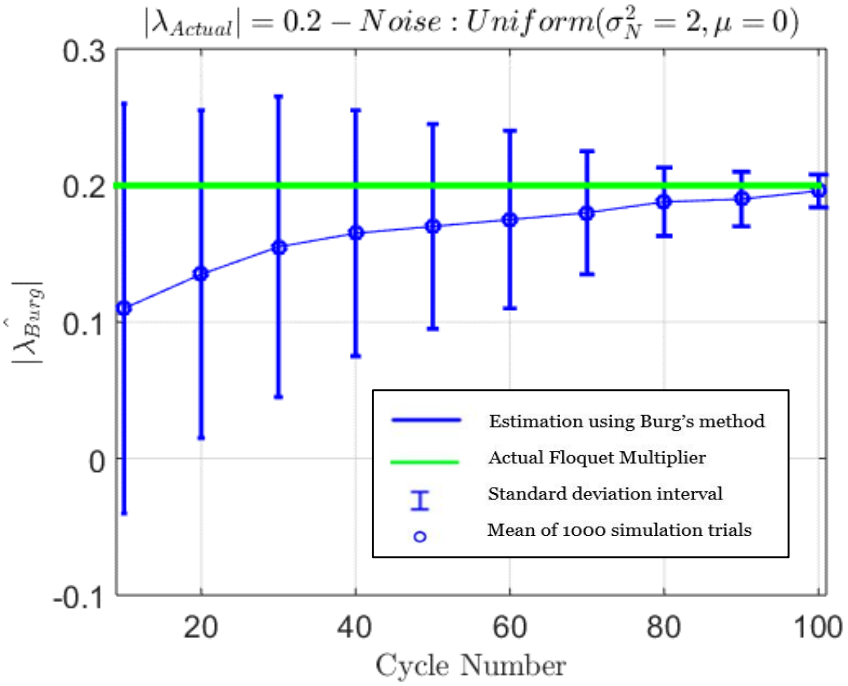

Figure 6. Burg's method estimation using noise from uniform distribution

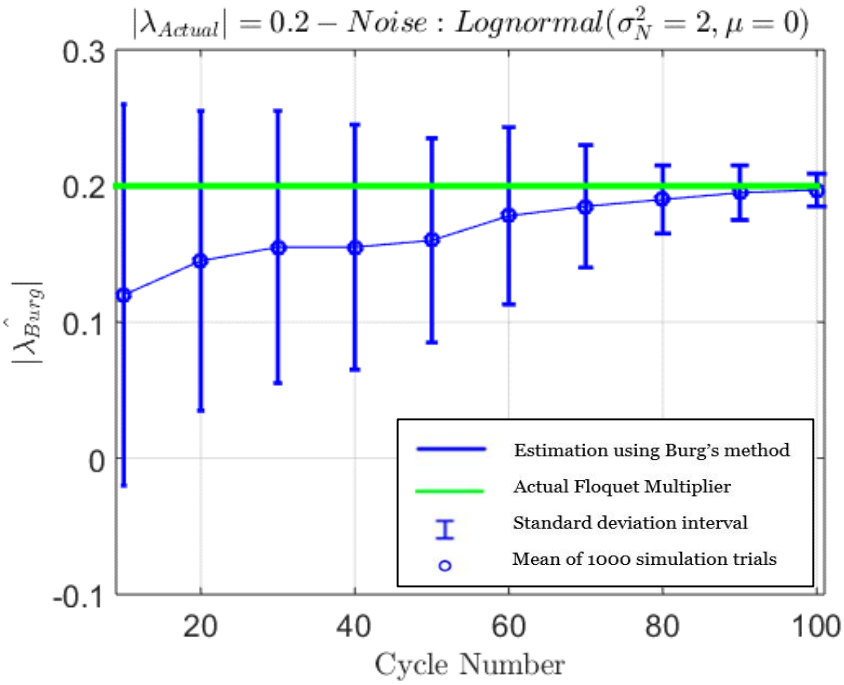

Figure 7. Burg's method estimation using noise from lognormal distribution

As shown in Figures 5,6 and 7, Burg's method can provide a little better estimation in comparison to Yule-Walker's method, but still the rate of convergence for this method is not acceptable.

Like the Yule-Walker's method, the estimation method of Burg has been evaluated by different values of Floquet multipliers. The results in the following figures show and confirm the existence of bias for larger values of Floquet multiplier for Burg's method.

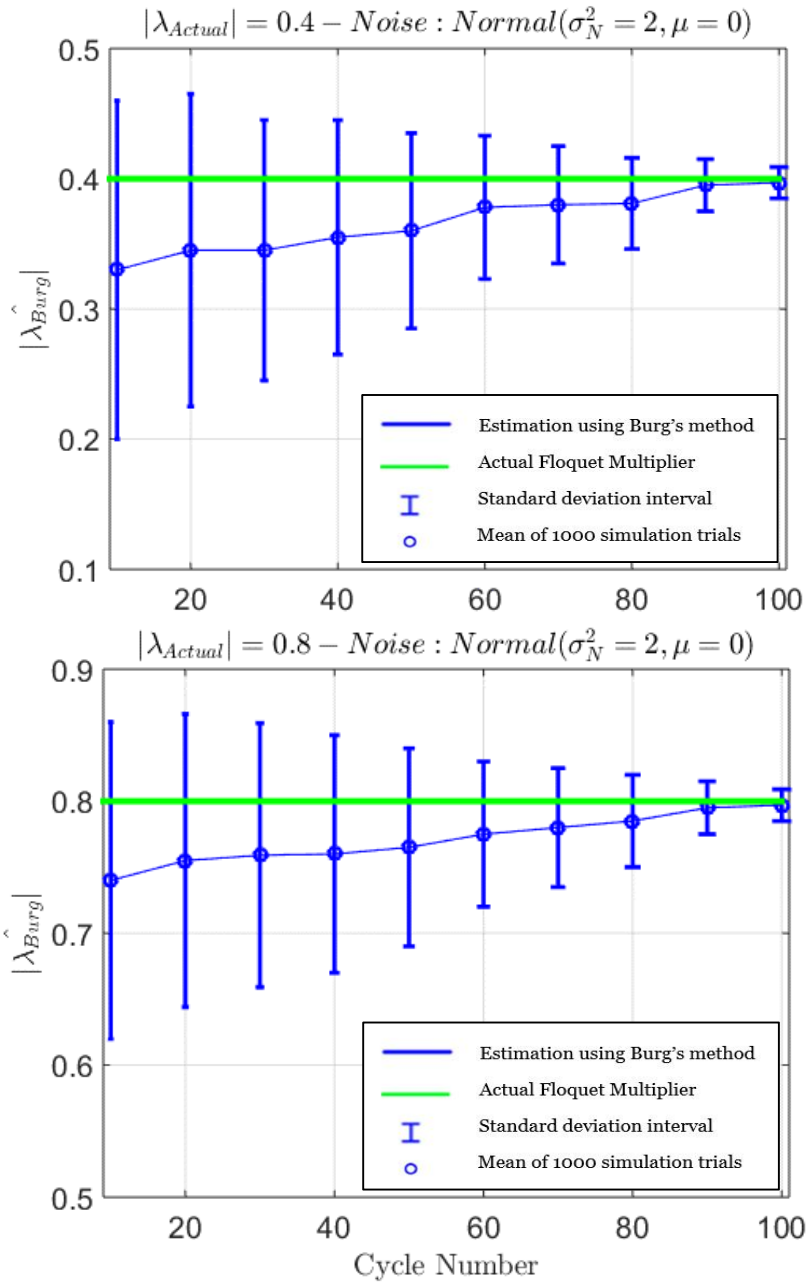

Figure 8. Burg's method estimation using noise from a normal distribution for different values of Floquet multiplier

3.2 Improved bias reduced methods

In order to estimate the Floquet multipliers and assess the orbital stability, Hurmuzlu et. al. and Dingwell et. al. used conventional methods such as Yule-Walker or other linear regression methods like least squares [7, 26].

The bias of the previous approaches was evaluated by numerical simulation for a one-dimensional case, which assures that the method would not be useful for higher dimensions. Also, Ahn and Hogan revealed that the common approach of estimating the Floquet multipliers by a least squares fit results in bias when the number of the cycles is not sufficiently large [1].

3.2.1 One-dimensional bias-reduction for Ahn's method

Ahn and Hogan used the property of the AR process and found the closed form approximation for the expectation of the bias [1].

$$E\left(\hat{\lambda}_{YW} - \lambda\right) \cong -\frac{1+\lambda}{M-1}\left(1 - \frac{1-\lambda^{M-1}}{(M-1)(1-\lambda)}\right). \tag{3.5}$$

Using properties of AR processes and assuming a sufficiently large number of cycles, the expected bias is approximately:

$$E\left(\hat{\lambda}_{YW} - \lambda\right) \cong -\left(\frac{\lambda^3 - \lambda^{2M+1}}{(M-1)(1-\lambda^2)}\right). \tag{3.6}$$

Ahn showed that the expected bias is approximately proportional to 1/n, but it does not depend on the noise level based on Eq. (3.6) [1]. He proposed the new estimator based on that:

$$\lambda_{Ahn} = \hat{\lambda}_{YW} + \left(\frac{\hat{\lambda}_{Burg}^3 - \hat{\lambda}_{Burg}^{2M+1}}{(M-1)\left(1-\hat{\lambda}_{Burg}^2\right)}\right). \tag{3.7}$$

where $\hat{\lambda}_{Burg}$ is the estimate from Burg's method. The true λ on the right hand side of Eq. (3.6) is unknown and therefore is replaced with an estimate. For the adjustment term, he chose Burg's estimation because this method guarantees stability of the estimated AR model [1]. Also, the uncorrected estimate is based on Yule-Walker's method, because its simplicity enables ready derivation of the bias and any necessary adjustment in closed form [1].

The generated time series and the estimated values of the Yule-Walker's and Burg's methods have been saved and used for the Ahn's method. We used different noise distributions to evaluate this method. Also, different Floquet multipliers have been used to assess the method.

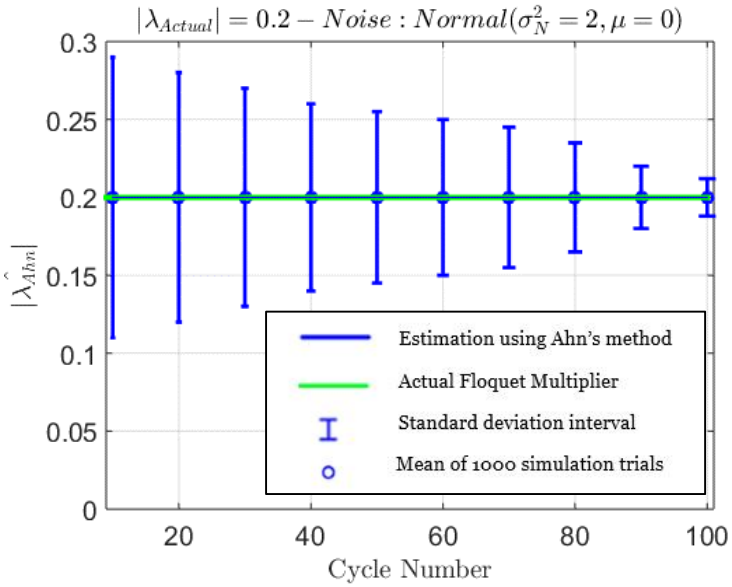

Figure 9. Ahn's method estimation using noise from normal distribution

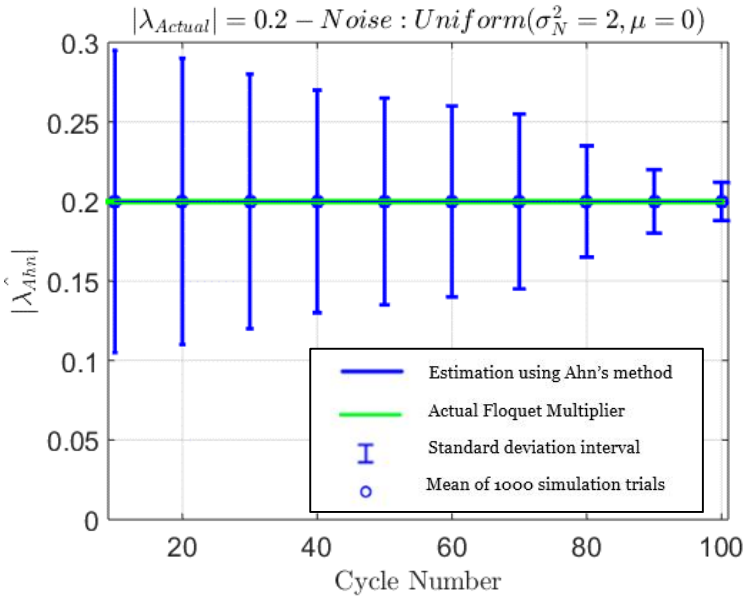

Figure 10. Ahn' method estimation using noise from uniform distribution

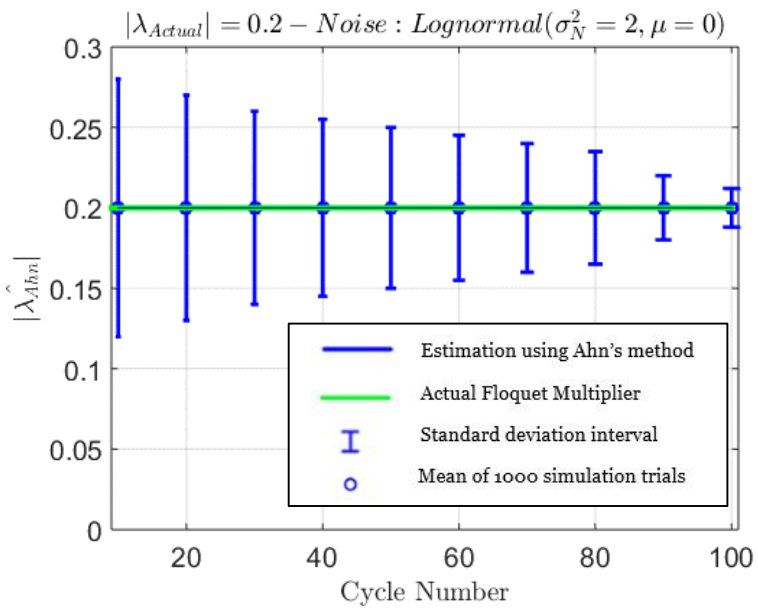

Figure 12. Ahn' method estimation using noise from lognormal distribution

Upon reviewing the simulation results using Ahn's method, we observe that the bias reduction process was successful. The results from Figure 9, 10 and 11 shows the independency of Ahn's method to the noise distribution.

The amount of bias for each of the methods discussed have been calculated and recorded to show the different methods' accuracy, in the following tables. In all of the tables, bias is $|\hat{\lambda}_{estimated} - \lambda_{actual}|$

Table 1. The bias of different one-dimensional estimation methods - normal noise distribution

Noise from normal distribution											
		Cycle length, M									
FM	**Method**	**10**	**20**	**30**	**40**	**50**	**60**	**70**	**80**	**90**	**100**
0.2	YW	517.6	508.1	432.3	390.8	331.5	231.4	122.8	81.9	31.2	19.5
0.2	Burg	515.8	522.4	428.4	414.1	319.2	215.1	112.7	68.5	52.6	15.2
0.2	Ahn	26.5	22.1	16.8	13.2	11.2	7.7	4.7	4.2	3.5	2.7
		*** Values are multiplied by 10000 for more clarification**									

Table 2. The bias of different one-dimensional estimation methods - uniform noise distribution

Noise from uniform distribution											
		Cycle length, M									
FM	**Method**	**10**	**20**	**30**	**40**	**50**	**60**	**70**	**80**	**90**	**100**
0.2	YW	539.7	521.1	437.4	425.8	337.5	235.1	129.7	89.5	39.7	29.5
0.2	Burg	525.8	521.4	429.4	424.1	329.2	225.1	111.7	65.5	39.6	29.2
0.2	Ahn	24.5	20.1	14.8	12.2	10.2	8.1	6.4	4.1	3.4	2.3
		*** Values are multiplied by 10000 for more clarification**									

Table 3. The bias of different one-dimensional estimation methods - uniform noise distribution

Noise from lognormal distribution											
		Cycle length, M									
FM	**Method**	**10**	**20**	**30**	**40**	**50**	**60**	**70**	**80**	**90**	**100**
0.2	YW	547.7	519.1	434.1	429.7	338.5	232.4	122.7	87.5	31.7	20.5
0.2	Burg	527.8	515.4	420.4	382.1	321.2	228.1	119.7	69.5	49.6	19.2
0.2	Ahn	26.5	22.1	19.8	12.8	11.2	9.9	6.7	3.2	2.8	2.1
		*** Values are multiplied by 10000 for more clarification**									

3.2.2 Multi-dimensional decomposition method

As observed from the results of Ahn's method, the reduced bias method works really well in assessing the orbital stability using estimation of Floquet multiplier. The extension of the method to the multi-dimensional case would be the next challenge as most of the experiments especially on human locomotion would require analysis of a multi-dimensional return map and different Floquet multipliers.

The idea of multi-dimensional case study comes from the matrix decomposition and theory of matrix functions [29].

As mentioned previously in the analysis of the return map:

$$S_{K+1} - S^* = J(S^*)[S_K - S^*] + \Delta_{K+1} \qquad K = 1,2,\dots,M \quad . \tag{3.8}$$

Also, the term X_{K+1} is the substituted form of $S_{K+1} - S^*$ as next state representation for the return map:

$$X_{K+1} = JX_K + \Delta_{K+1} \qquad K = 1,2,\dots,M \quad . \tag{3.9}$$

Using the Yule-Walker method, Jacobian matrix could be estimated primarily. We call this estimation $\hat{J}_{YW}$. From the Jordan canonical form and estimated eigenvalues of the $\hat{J}_{YW}$ called $\hat{\lambda}_{YW}$ we can find the Jordan canonical form by assuming that the eigenvalues are not the equal value in order to extend the concept to more general cases [7]:

$$\hat{J}_{YW} = P^{-1} * \hat{J}_{block-YW} * P \qquad . \tag{3.10}$$

where P is the transformation matrix and $\hat{J}_{block-YW}$ is $\mathrm{K} \times \mathrm{K}$ estimated decomposed matrix. As we know the canonical Jordan form assuming the eigenvalues are not equal and Jordan block is based on absolute values of eigenvalues would have 1×1 blocks of eigenvalues making a diagonal block with eigenvalues:

$$\hat{J}_{block-YW} = \begin{bmatrix} \hat{\lambda}_{1,YW} & \cdots & 0 \\ \vdots & \ddots & \vdots \\ 0 & \cdots & \hat{\lambda}_{K,YW} \end{bmatrix} \quad . \tag{3.11}$$

In Eq. (3.11), the estimated values of Floquet multipliers need to be bias-reduced. The matrix function via Jordan canonical form allows:

$$f(\hat{J}_{YW}) = P^{-1} * f(\hat{J}_{block-YW}) * P \quad , \tag{3.12}$$

$$f(\hat{J}_{block-YW}) = P * f(\hat{J}_{YW}) * P^{-1} \quad , \tag{3.13}$$

So, it means any function took over Jacobian matrices can be applied to canonical form as well. In order to reduce the bias for the both Jacobian forms, we could use the Ahn's method as described properly for the one-dimensional case studies.

Assuming the eigenvalues are not the same and the noises are independent in each channel, we can reduce the bias as the following function over Jordan canonical form as Bias Reduced (BR):

$$\hat{J}_{block-YW-BR} = \begin{bmatrix} \lambda_{1,bias-reduced} & \cdots & 0 \\ \vdots & \ddots & \vdots \\ 0 & \cdots & \lambda_{K,bias-reduced} \end{bmatrix} \rightarrow$$
$$= \begin{bmatrix} \lambda_{1,YW} + \dfrac{\hat{\lambda}_{1,Burg}^{3} + \hat{\lambda}_{1,Burg}^{2M+1}}{(M-1)(1-\hat{\lambda}_{1,Burg}^{2})} & \cdots & 0 \\ \vdots & \ddots & \vdots \\ 0 & \cdots & \lambda_{K,YW} + \dfrac{\hat{\lambda}_{K,Burg}^{3} + \hat{\lambda}_{K,Burg}^{2M+1}}{(M-1)(1-\hat{\lambda}_{K,Burg}^{2})} \end{bmatrix} \tag{3.14}$$

As the method is a vectored type bias adjusted of Yule-Walker's method, we decided to call it Vector Adjusted Ahn-Hogan (VAAH). The eigenvalues in $\hat{J}_{block-YW-BR}$ (Eq. (3.14)) are bias reduced.

The summary of VAAH method can be reviewed in the following steps:

Algorithm: **Vector Adjusted Ahn-Hogan (VAAH) Method**

1: Using the Yule-Walker and Burg's methods, evaluate the Jacobian matrix for a VAR model in Eq. (3.9). Denote the estimates as $\hat{J}_{YW}$ and $\hat{J}_{Burg}$.

2: Calculate the estimated eigenvalues of $\hat{J}_{YW}$ and find decomposition transformation matrix P.

3: Using the transformation matrix P, find the block canonical form of $\hat{J}_{YW}$ using $\hat{J}_{block-YW} = P * \hat{J}_{YW} * P^{-1}$. Denote the Jacobian canonical form estimate $\hat{J}_{block-YW}$.

4: Using the bias-reduction formula based on Ahn's method, reduce the bias of each of the individual eigenvalues:

$$\hat{J}_{block-YW-BR} = \begin{bmatrix} \lambda_{1,bias-reduced} & \cdots & 0 \\ \vdots & \ddots & \vdots \\ 0 & \cdots & \lambda_{K,bias-reduced} \end{bmatrix} \rightarrow$$

$$= \begin{bmatrix} \lambda_{1,YW} + \dfrac{\hat{\lambda}^3_{1,Burg} + \hat{\lambda}^{2M+1}_{1,Burg}}{(M-1)(1-\hat{\lambda}^2_{1,Burg})} & \cdots & 0 \\ \vdots & \ddots & \vdots \\ 0 & \cdots & \lambda_{K,YW} + \dfrac{\hat{\lambda}^3_{K,Burg} + \hat{\lambda}^{2M+1}_{K,Burg}}{(M-1)(1-\hat{\lambda}^2_{K,Burg})} \end{bmatrix}$$

5: Calculate the bias-reduced Floquet multipliers using the updated eigenvalues of $\hat{J}_{block-YW-BR}$

The simulation results for the multi-dimensional return map would show the accuracy of the estimations. To this end, we used a two-dimensional return map with generated time series like the one-dimensional case.

$$J = \begin{bmatrix} 0.2 & 0.01 \\ 0.4 & 0.85 \end{bmatrix} \ , \Sigma_{\Delta} = \begin{bmatrix} 4 & 0 \\ 0 & 4 \end{bmatrix}, \tag{3.15}$$

$$|\lambda_1| = 0.1939 \quad , \quad |\lambda_2| = 0.8631 \ , \tag{3.16}$$

which Σ_{Δ} is the covariance matrix of the noise from different distributions with zero mean. Also, in all of the figures $|.|$ shows the absolute values of eigenvalues.

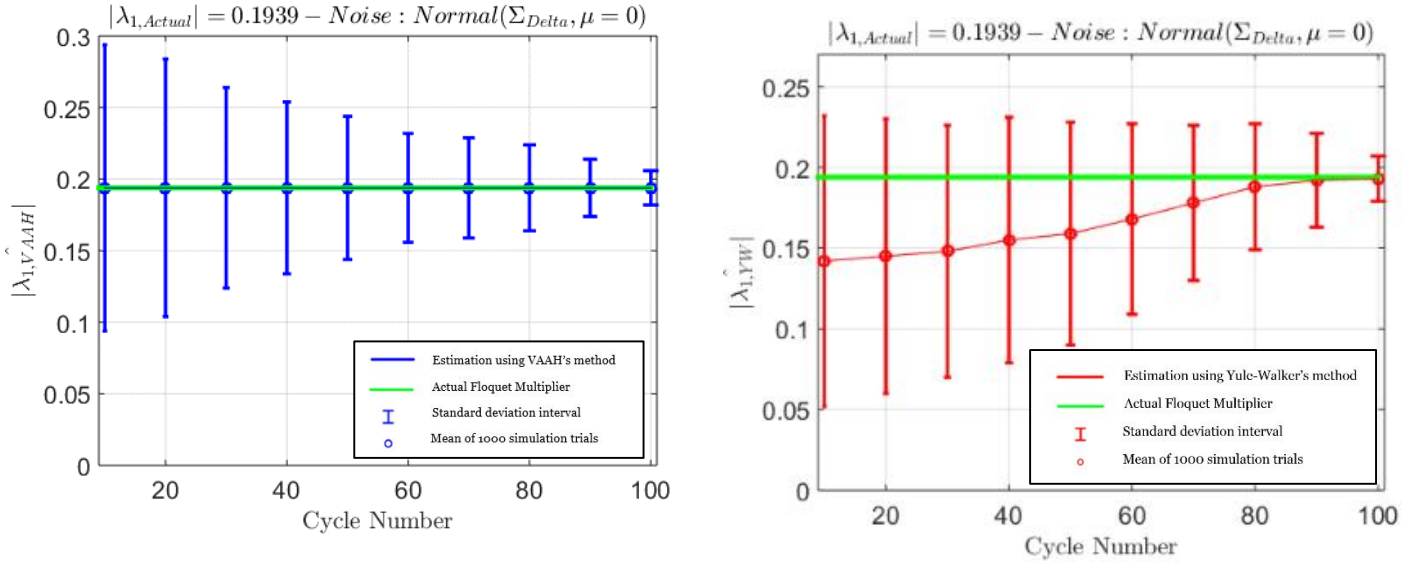

Figure 13. Yule-Walker's (left) and VAAH's (right) methods estimation using noise from normal distribution –first bias-reduced eigenvalue results

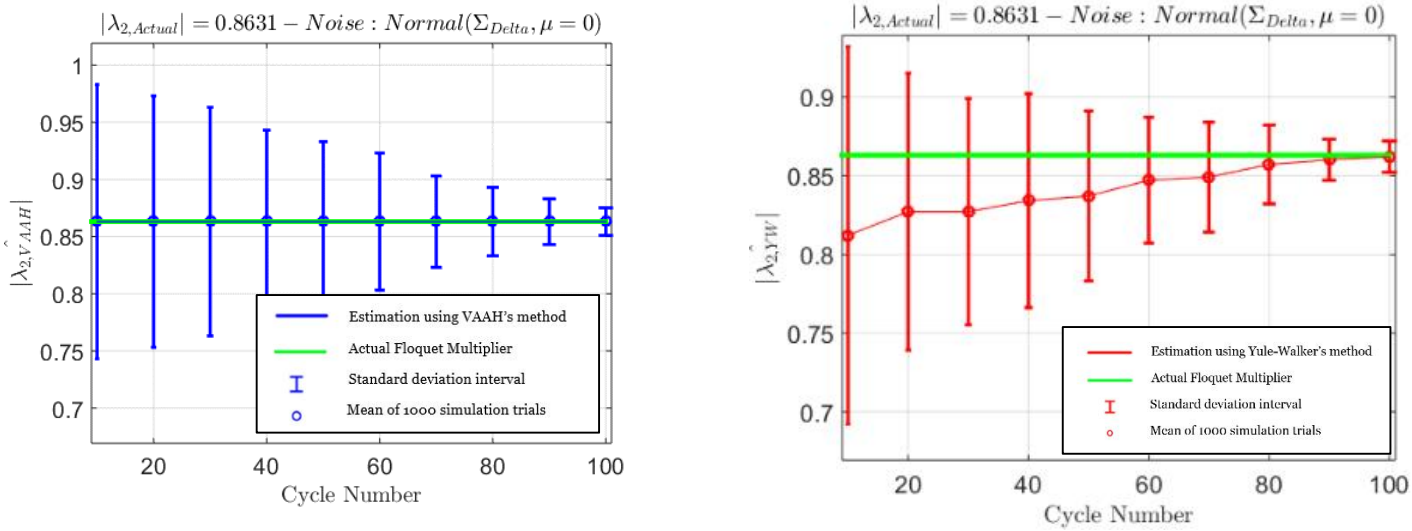

Figure 14. Yule-Walker's (left) and VAAH's (right) methods estimation using noise from normal distribution –second bias-reduced eigenvalue results

The figures 12 and 13 shows the Yule-Walker's and VAAH's method results for a normal noise with Σ_Δ as covariance matrix and zero mean.

The bias has been reduced for each of the individual eigenvalues of Jacobian matrix and the variance of the estimations decreases by increment of cycles. The method has been evaluated by different noise distributions.

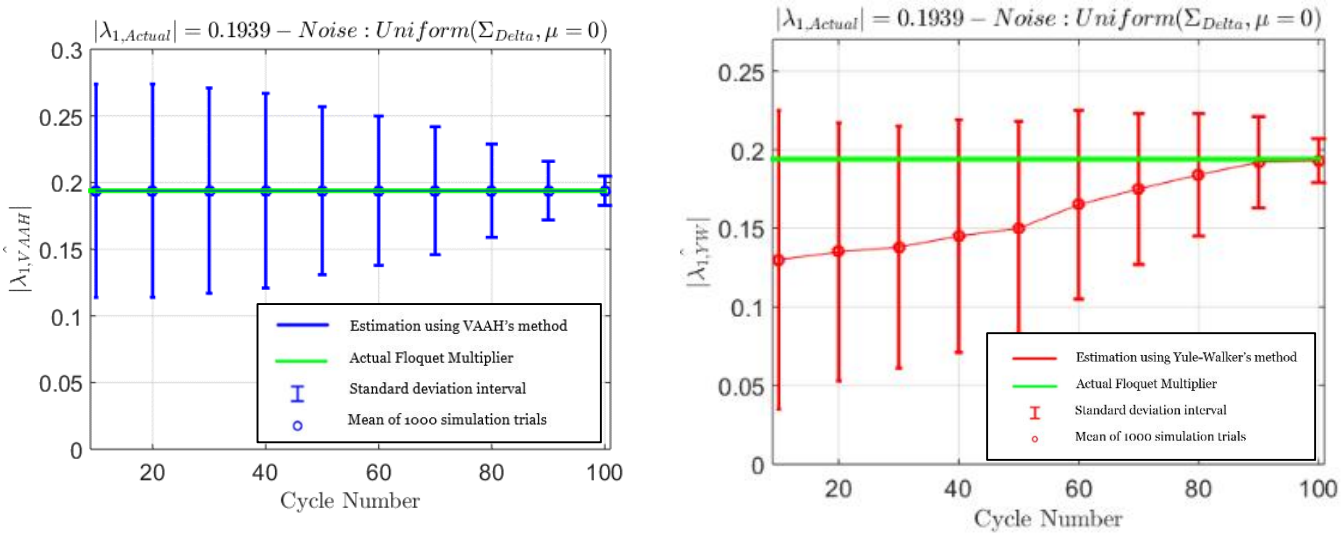

Figure 15. Yule-Walker's (left) and VAAH's (right) methods estimation using noise from uniform distribution –first bias-reduced eigenvalue results

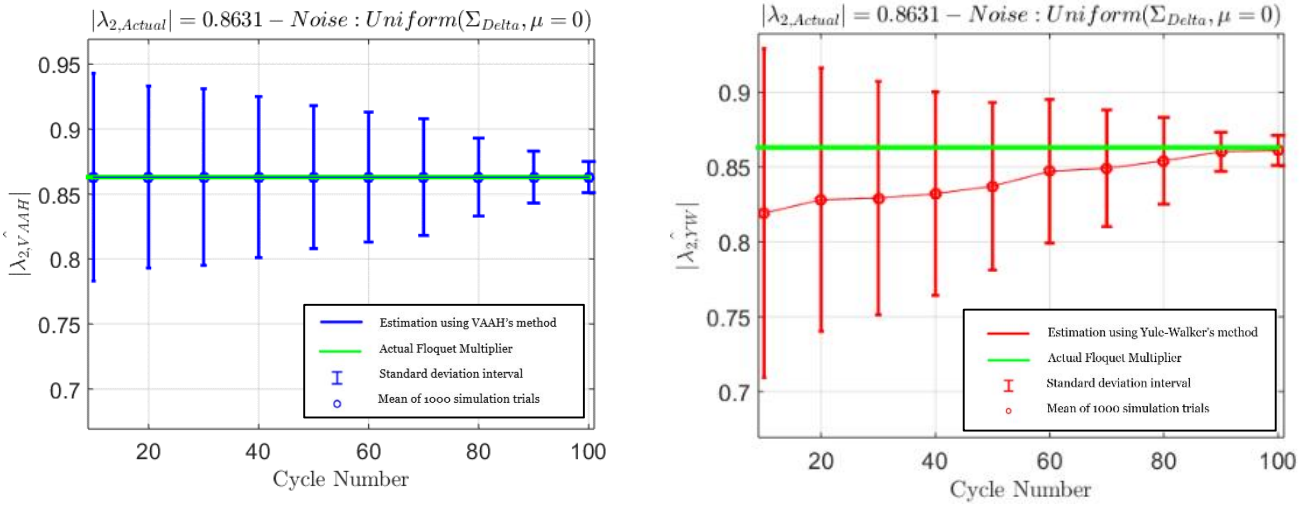

Figure 16. Yule-Walker's (left) and VAAH's (right) methods estimation using noise from uniform distribution –second bias-reduced eigenvalue results

The results of noise from uniform distribution confirms the independency of the method with noise distribution type. The lognormal noise distribution results have been tested as well.

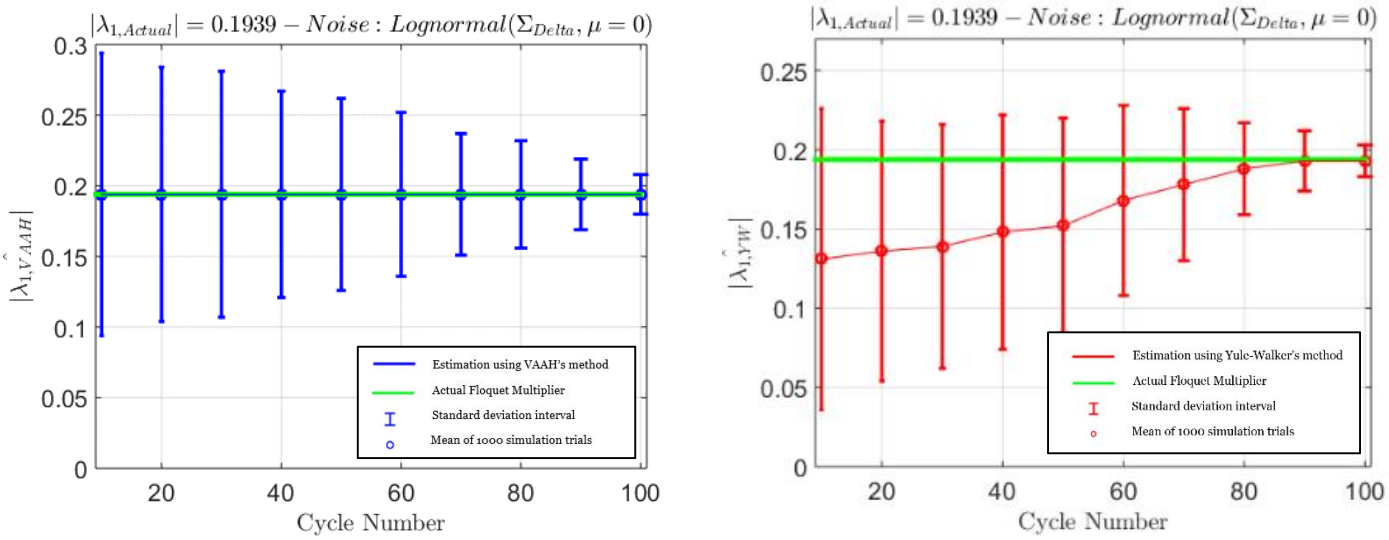

Figure 17. Yule-Walker's (left) and VAAH's (right) methods estimation using noise from lognormal distribution –first bias-reduced eigenvalue results

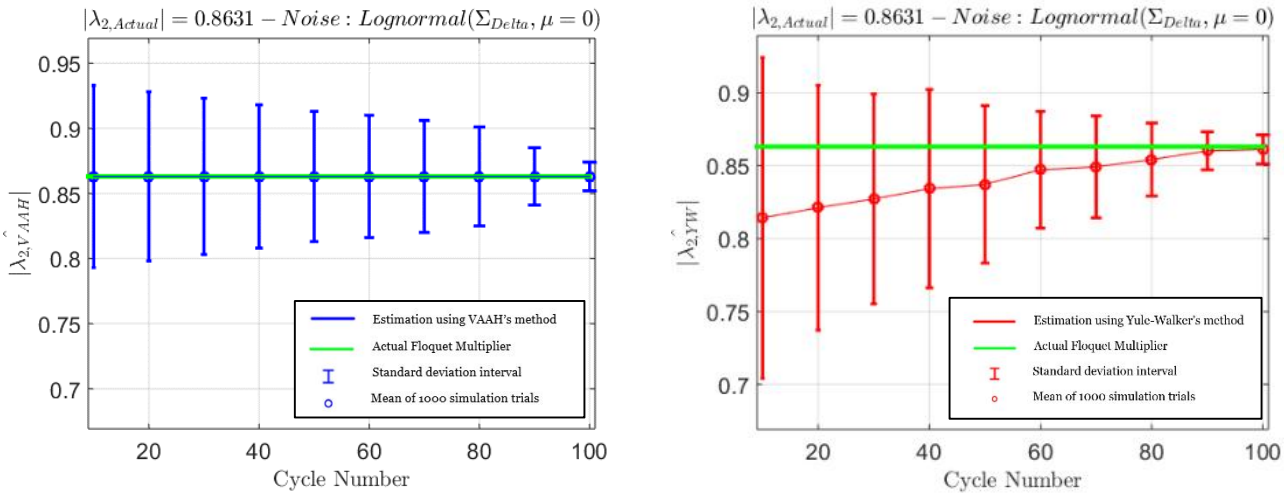

Figure 18. Yule-Walker's (left) and VAAH's (right) methods estimation using noise from lognormal distribution – second bias-reduced eigenvalue results

As it is shown in the figures, the new bias-reduction algorithm is not dependent to the noise distribution and only with different standard deviations finds the true values of Floquet multipliers.

The followings show the results for the Burg's method compared with new method VAAH for the two-dimensional return map with different noise distribution.

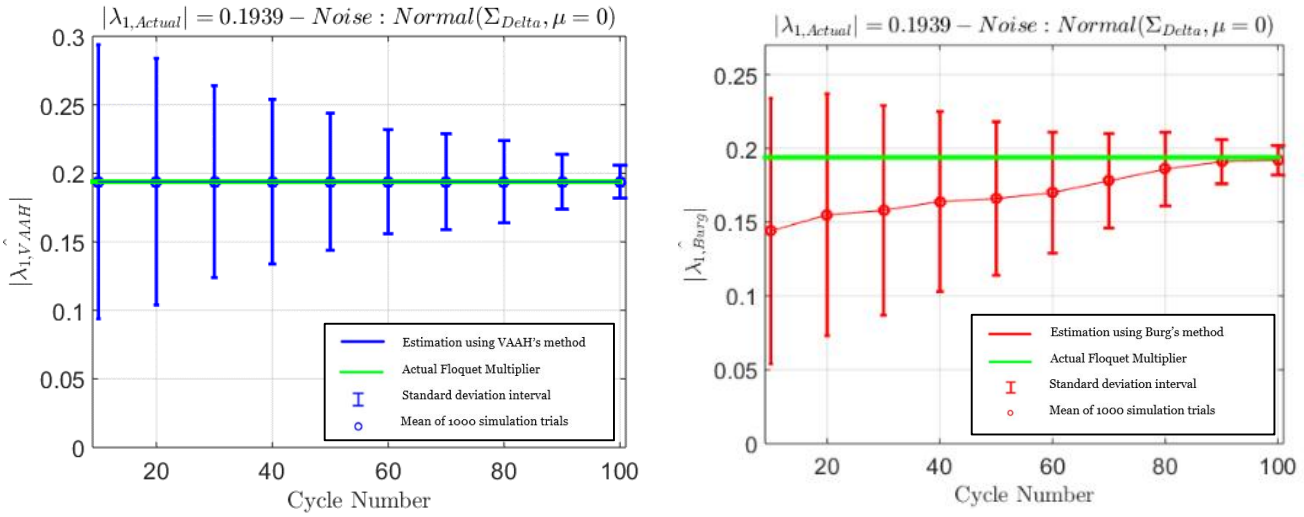

Figure 19. Burg's (left) and VAAH's (right) methods estimation using noise from normal distribution – first bias-reduced eigenvalue results

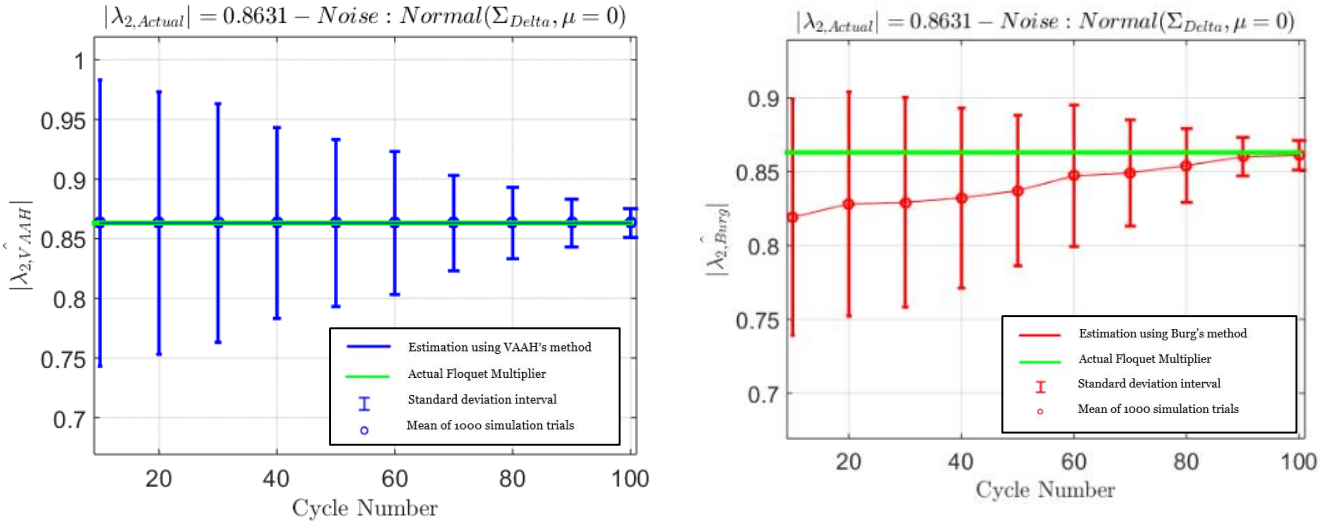

Figure 20. Burg's (left) and VAAH's (right) methods estimation using noise from normal distribution – first bias-reduced eigenvalue results

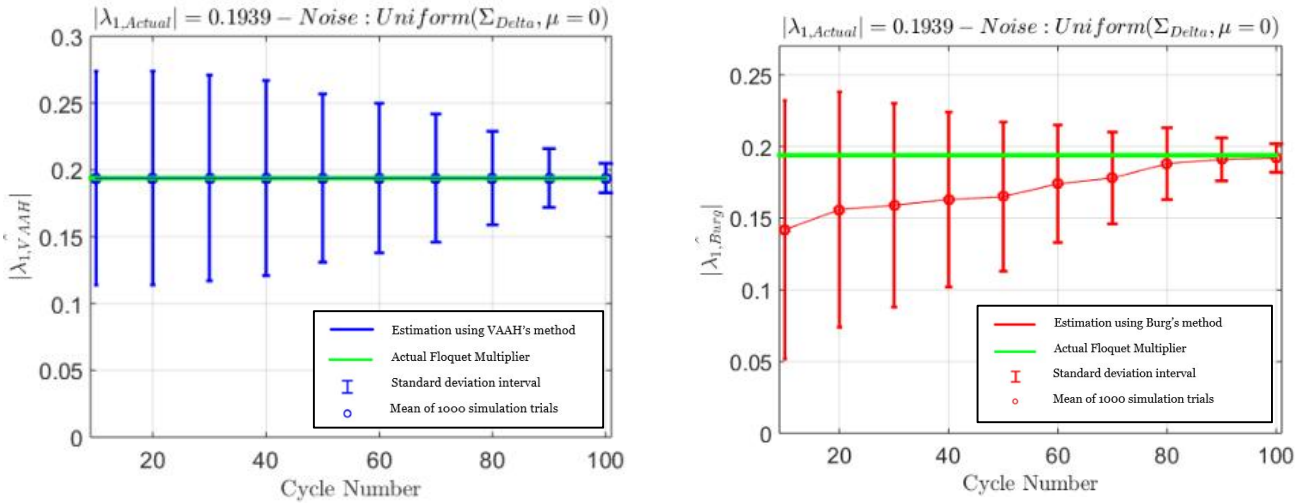

Figure 21. Burg's (left) and VAAH's (right) methods estimation using noise from uniform distribution – second bias-reduced eigenvalue results

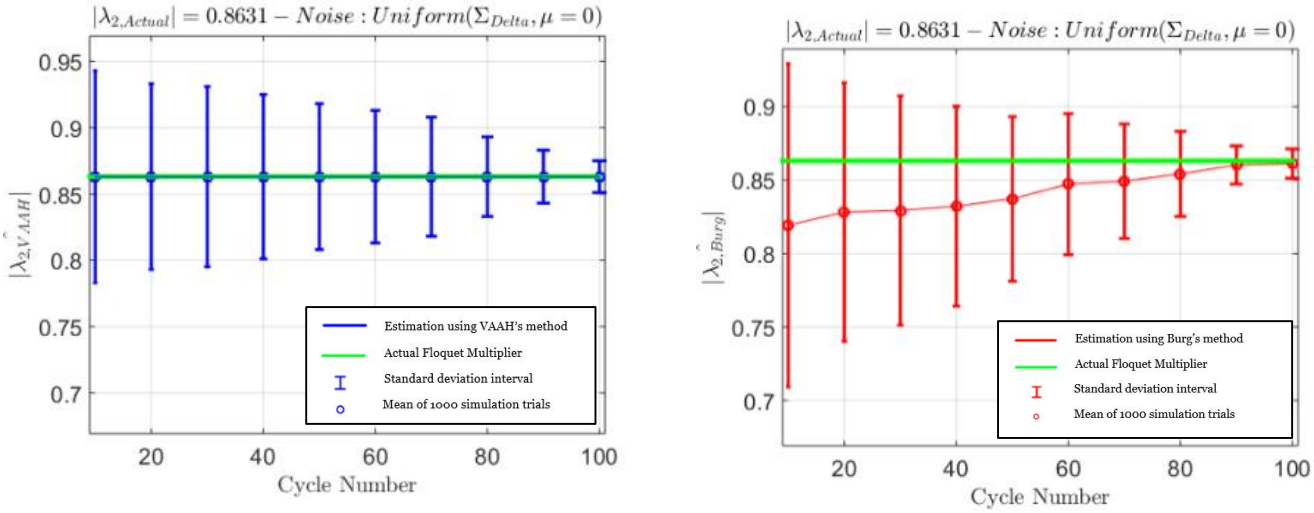

Figure 22. Burg's (left) and VAAH's (right) methods estimation using noise from uniform distribution – second bias-reduced eigenvalue results

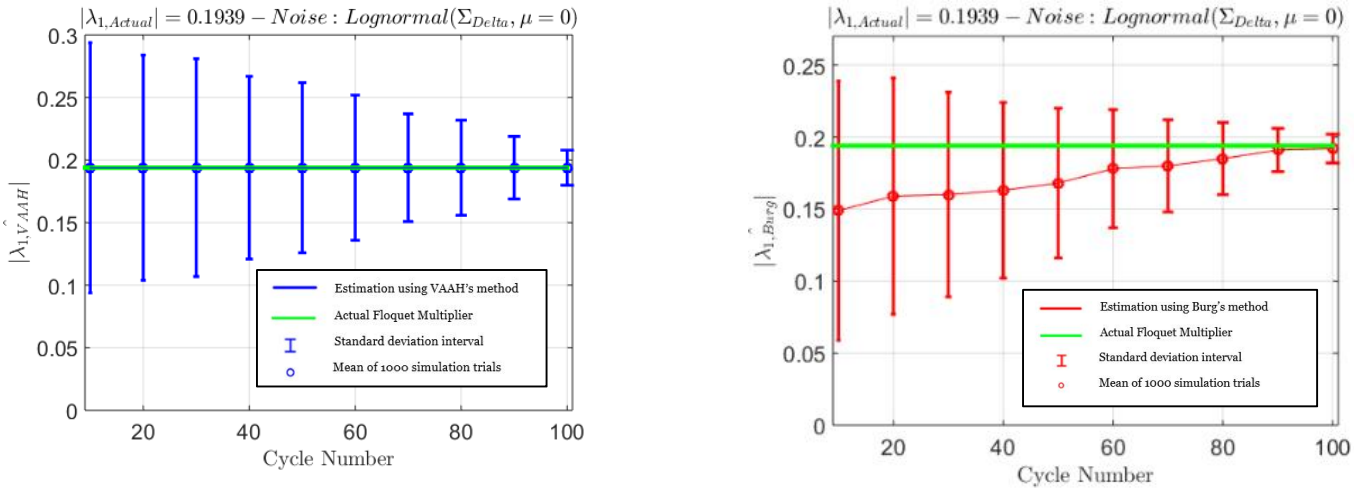

Figure 23. Burg's (left) and VAAH's (right) methods estimation using noise from lognormal distribution – first bias-reduced eigenvalue results

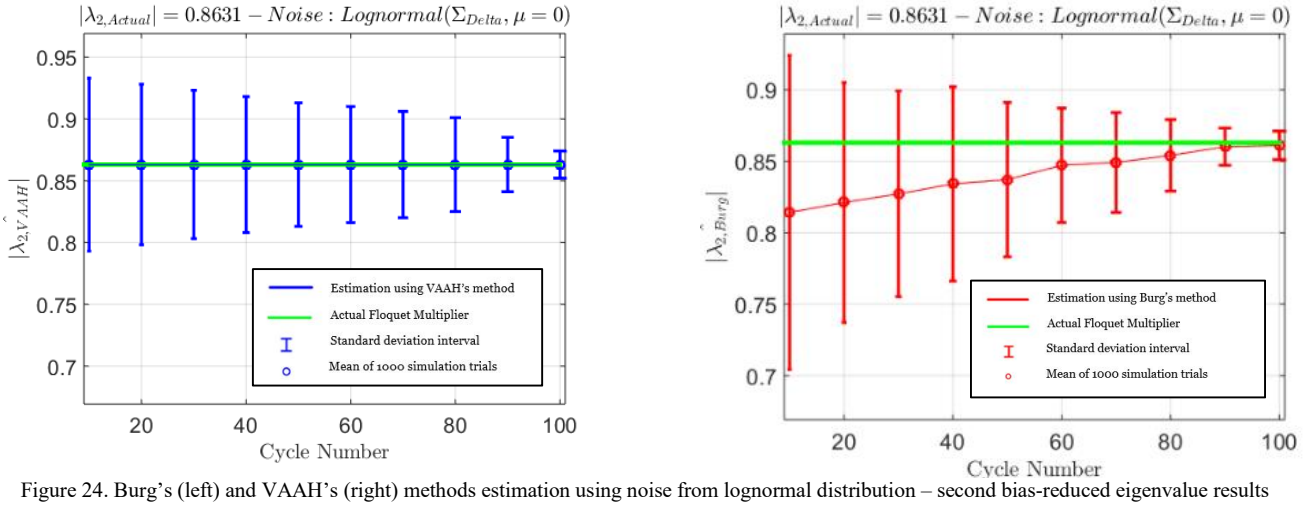

Figure 24. Burg's (left) and VAAH's (right) methods estimation using noise from lognormal distribution – second bias-reduced eigenvalue results

Table 4. The bias of different two-dimensional estimation methods - normal noise distribution

Noise from normal distribution											
		Cycle length, M									
FM	**Method**	**10**	**20**	**30**	**40**	**50**	**60**	**70**	**80**	**90**	**100**
0.1939	YW	527.7	509.1	439.4	429.8	339.5	239.4	129.7	89.5	39.7	29.5
0.1939	Burg	525.8	521.4	429.4	424.1	329.2	225.1	111.7	65.5	39.6	29.2
0.1939	VAAH	24.5	20.1	14.8	12.2	10.2	7.7	6.7	4.2	3.8	1.7
0.8631	YW	519.3	318.5	316.5	313.8	241.7	131.5	121.5	111.9	51.1	21.2
0.8631	Burg	517.1	511.5	416.7	401.2	231.7	121.8	111.1	101.8	21.9	16.4
0.8631	VAAH	21.4	16.1	14.2	12.5	10.8	6.8	4.5	3.6	2.7	1.8
		*** Values are multiplied by 10000 for more clarification**									

Table 5. The bias of different two-dimensional estimation methods - uniform noise distribution

Noise from uniform distribution											
		Cycle length, M									
FM	**Method**	**10**	**20**	**30**	**40**	**50**	**60**	**70**	**80**	**90**	**100**
0.1939	YW	627.8	524.7	519.5	514.4	439.5	339.4	139.9	85.3	69.1	39.2
0.1939	Burg	521.5	419.2	414.6	409.9	404.4	323.4	224.1	129.9	58.2	19.1
0.1939	VAAH	29.2	25.5	19.6	15.2	13.2	10.7	9.7	8.4	6.2	3.2
0.8631	YW	519.1	418.3	416.5	331.8	221.4	131.6	121.1	111.2	61.7	21.5
0.8631	Burg	417.6	318.5	316.2	221.4	216.2	131.1	123.7	111.5	46.1	19.7
0.8631	VAAH	26.4	21.2	19.7	17.8	15.2	11.3	10.7	8.9	5.2	2.8
		*** Values are multiplied by 10000 for more clarification**									

Table 6. The bias of different two-dimensional estimation methods - lognormal noise distribution

Noise from lognormal distribution											
		Cycle length, M									
FM	**Method**	**10**	**20**	**30**	**40**	**50**	**60**	**70**	**80**	**90**	**100**
0.1939	YW	627.2	621.4	524.6	434.7	430.9	331.4	227.2	120.1	89.3	53.1
0.1939	Burg	439.1	424.5	359.7	329.8	259.4	229.5	189.9	124.7	39.7	27.1
0.1939	VAAH	24.1	20.7	18.0	16.12	15.1	6.70	6.2	5.1	4.1	3.7
0.8631	YW	517.1	511.5	418.6	331.8	317.1	131.8	118.7	113.6	91.1	63.2
0.8631	Burg	519.7	419.9	319.5	213.1	211.3	131.4	121.7	111.9	71.2	41.0
0.8631	VAAH	31.1	25.3	24.1	20.1	18.1	15.1	14.1	7.7	6.4	1.8
		*** Values are multiplied by 10000 for more clarification**									

3.2.3 Walking model orbital stability

As an example of the high dimensional return map, we used the VAAH's method to assess the orbital stability of a walking model. The model is a point-feet five-link biped model and the motion dynamics are from research by Khazenifard et al. [3] .

The model is depicted in Fig. 18. The model consists of a trunk, two thigh and two shank segments. The model orientation was defined by joint angles $q = [q_1, q_2, q_3, q_4, q_5]$. This walking robot performed different consecutive strides. This simulation was performed using MATLAB (Math works Inc.).

In order to reconstruct the state-space equations for the analysis of orbital stability using a linearized Poincaré map, the kinematics data (joint angles and velocities) was obtained from the model. The noise was added to each of the gait cycles and to dynamics of motions of the walking model. Physical parameters used from Khazenifard et. al. about bipedal robot [30]. The robot body model is symmetric and $l_1 = l_2 = l_3 = 34.5\ cm$.

In order to obtain the actual Floquet multipliers of the model, we run the model for 300 strides with an initial perturbation to find the accurate and accepted Floquet multipliers for the comparison. The amount of perturbation used is comparable to the noise level conducted for each cycle.

Three distributions of noise (normal, uniform and lognormal) were generated and added to the walking model dynamics of the motion in each cycle. The Floquet multipliers were estimated for each time series (from 10 to 100) using both the least squares and the VAAH's method and then compared with actual Floquet multipliers obtained from the initial test

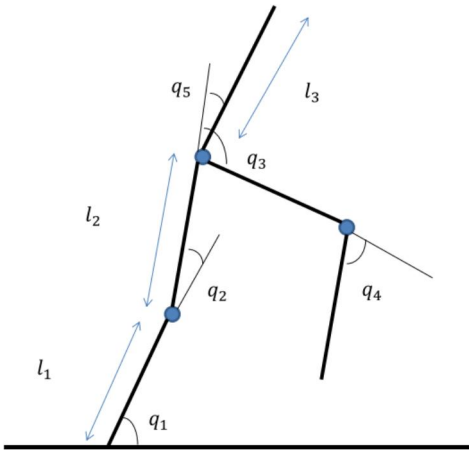

Figure 25. The Walking model in the sagittal plane

The state space $S_K = [q_{1K}, q_{2K}, q_{3K}, q_{4K}, q_{5K}, \dot{q}_{1K}, \dot{q}_{2K}, \dot{q}_{3K}, \dot{q}_{4K}, \dot{q}_{5K}] \in R^{10}$ which K is the stride numbers as defined in last chapter. Using the simulation studies and recording the kinematics data from each cycle number, Jacobian matrix and Floquet Multipliers are estimated for using both the least squares and VAAH's methods.

The robot walks for different stride numbers M ∈ {10,20,30,40,50,60,70,80,90,100}. The simulation results for the mean and the maximum Floquet multipliers (as those are absolute values of eigenvalues, either complex conjugate or real) are depicted in the following figures for different noise distributions.

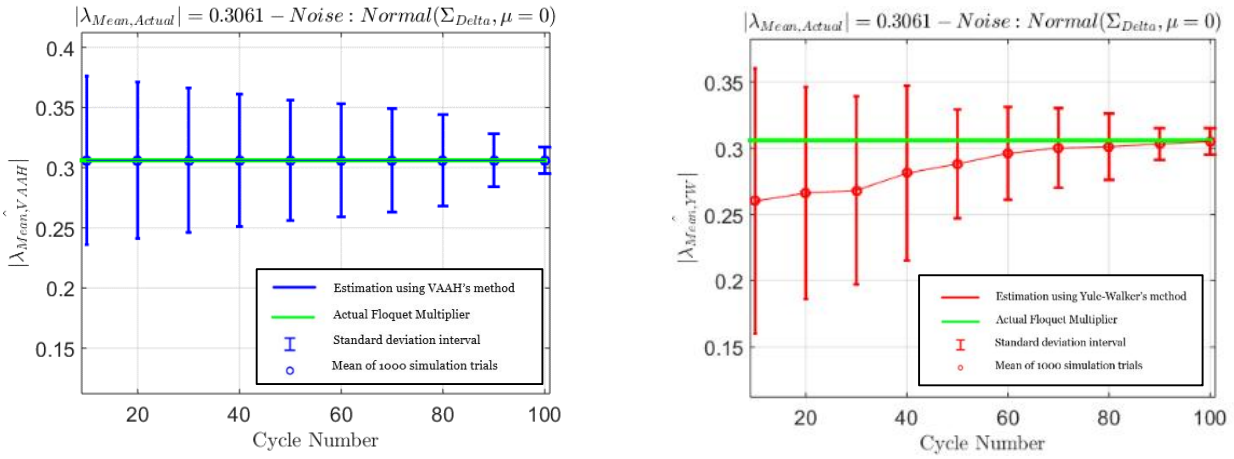

Figure 26. Walking model simulation, estimation of Floquet multipliers using Yule-Walker's (right) and VAAH's method (left) – Mean of Floquet multipliers with normal noise

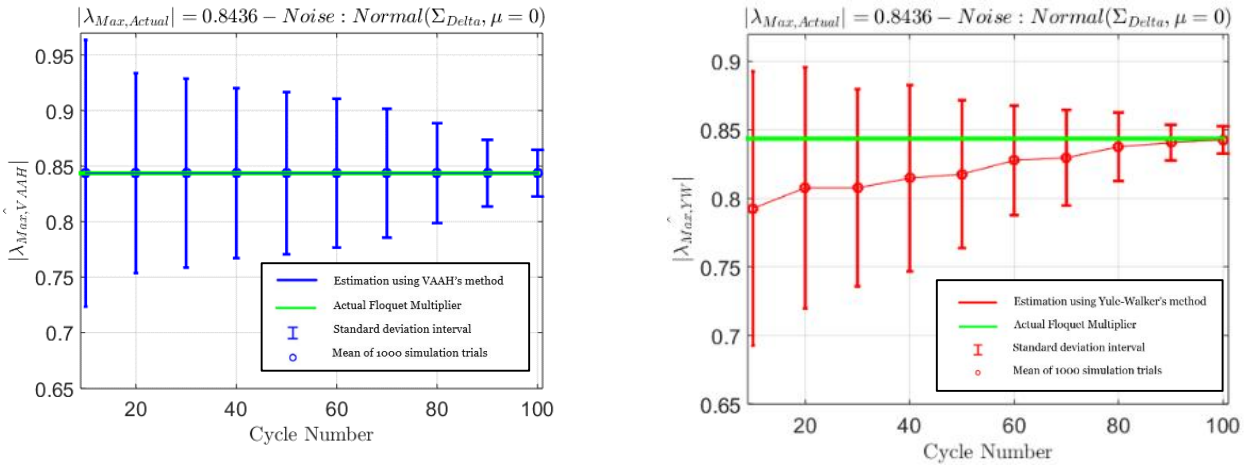

\

Figure 27. Walking model simulation, estimation of Floquet multipliers using Yule-Walker's (right) and VAAH's method (left) – Maximum of Floquet multipliers with normal noise

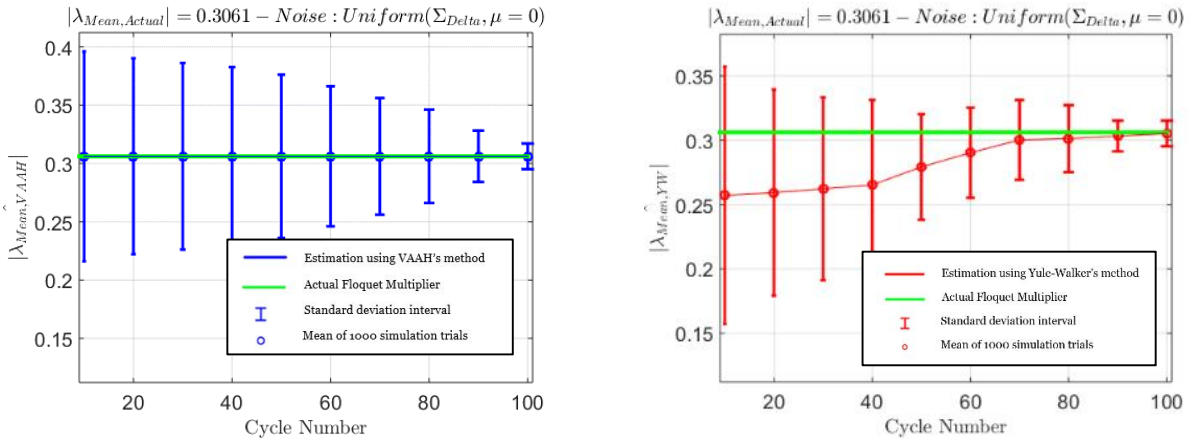

Figure 27. Walking model simulation, estimation of Floquet multipliers using Yule-Walker's (right) and VAAH's method (left)– Maximum of Floquet multipliers with lognormal noise

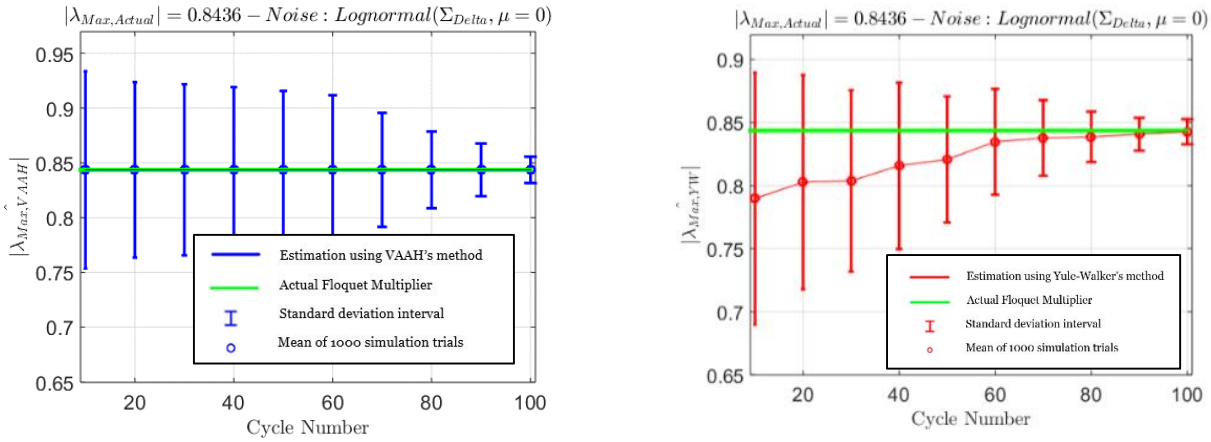

Figure 28. Walking model simulation, estimation of Floquet multipliers using Yule-Walker's (right) and VAAH's method (left)– Maximum of Floquet multipliers with uniform noise

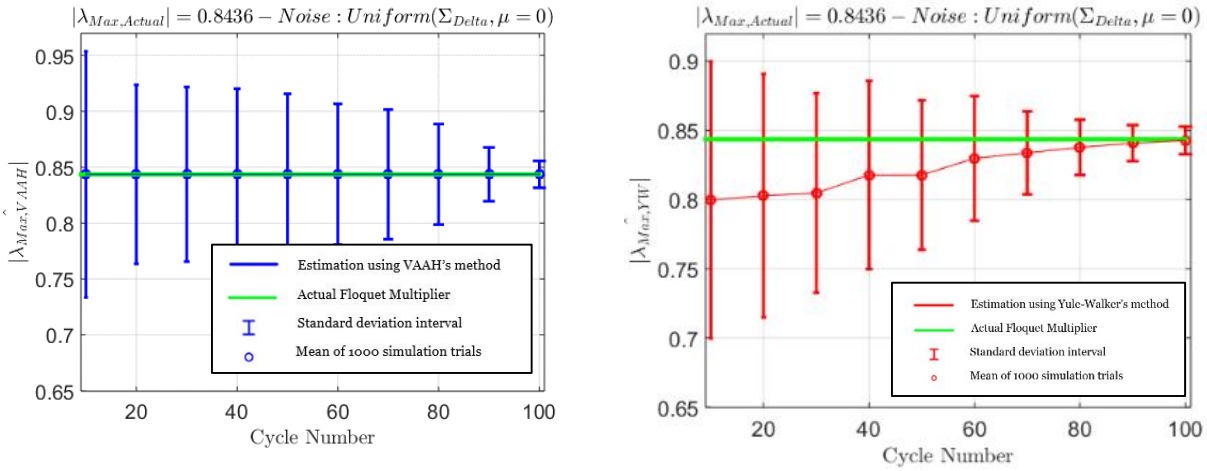

Figure 30. Walking model simulation, estimation of Floquet multipliers using Yule-Walker's (right) and VAAH's method (left)– Mean of Floquet multipliers with lognormal noise

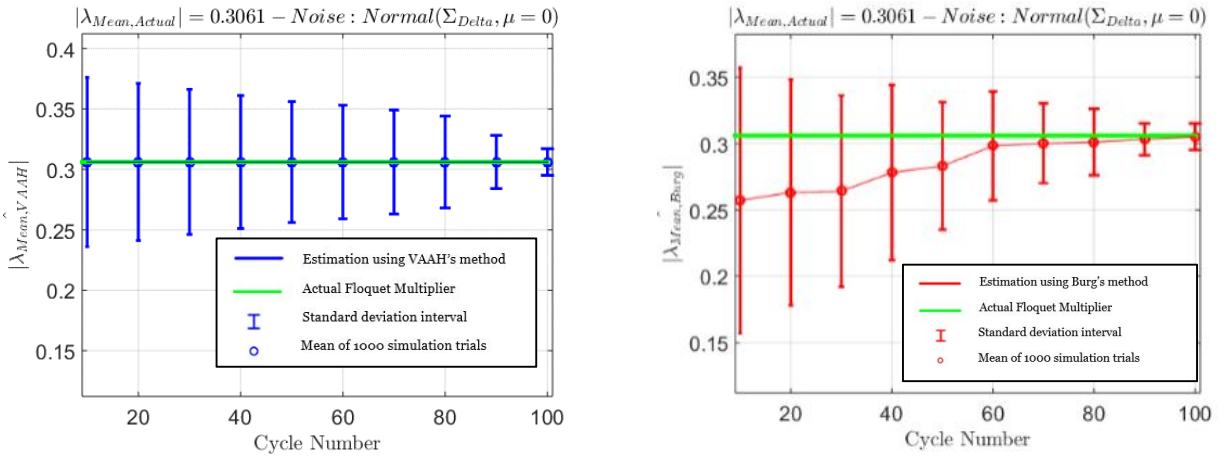

Figure 30. Walking model simulation, estimation of Floquet multipliers using Burg's (right) and VAAH's method (left)– Mean of Floquet multipliers with normal noise

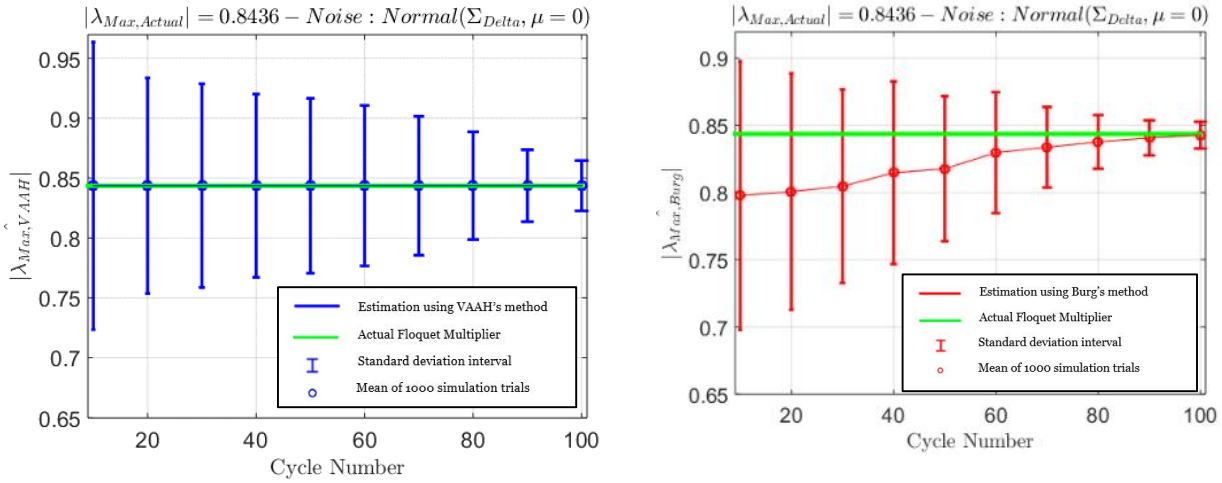

Figure 31. Walking model simulation, estimation of Floquet multipliers using Burg's (right) and VAAH's method (left)– Max of Floquet multipliers with normal noise

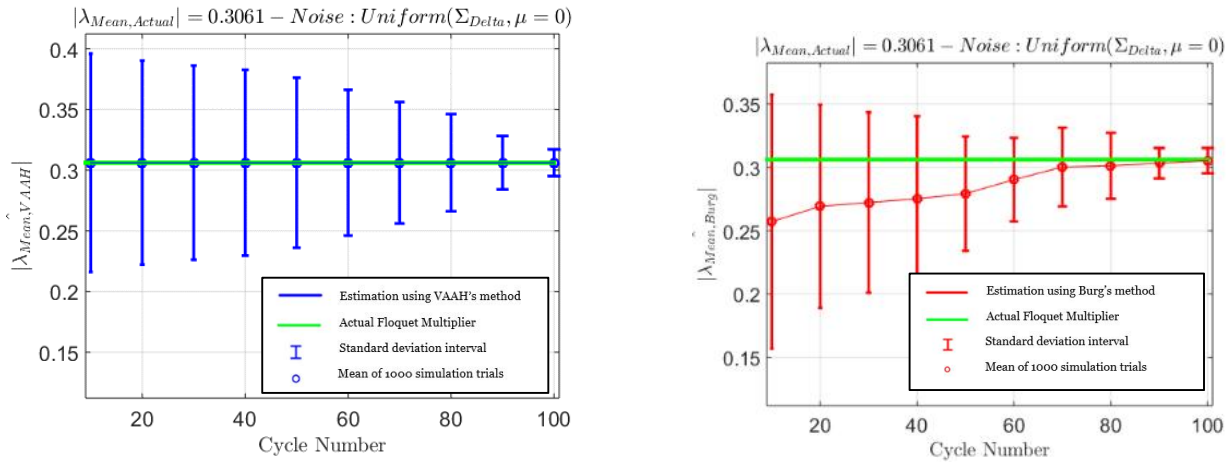

Figure 32. Walking model simulation, estimation of Floquet multipliers using Burg's (right) and VAAH's method (left)– Mean of Floquet multipliers with uniform noise

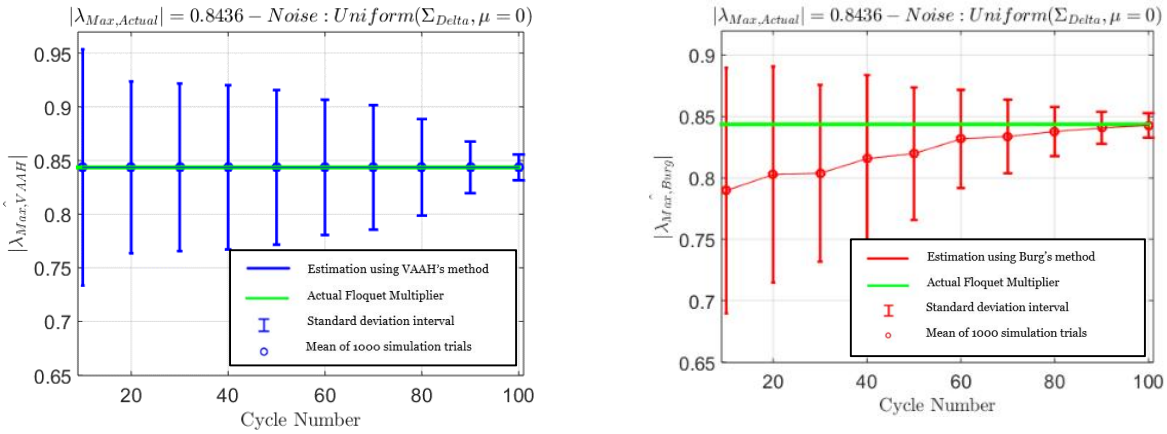

Figure 35. Walking model simulation, estimation of Floquet multipliers using Burg's (right) and VAAH's method (left)– Mean of Floquet multipliers with uniform noise

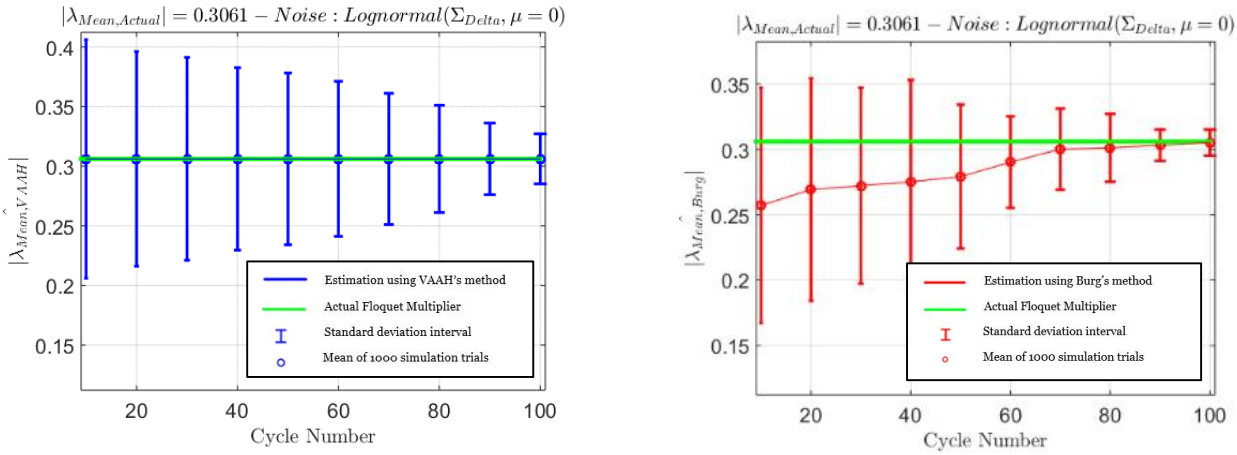

Figure 34. Walking model simulation, estimation of Floquet multipliers using Burg's (right) and VAAH's method (left)– Mean of Floquet multipliers with uniform noise

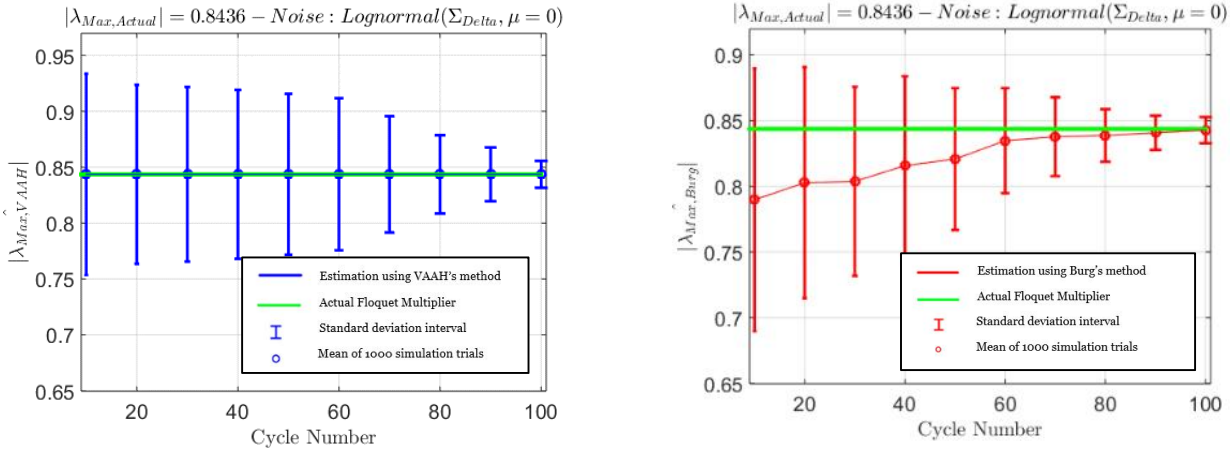

Figure 33. Walking model simulation, estimation of Floquet multipliers using Burg's (right) and VAAH's method (left)– Mean of Floquet multipliers with uniform noise

Table 7. The bias of different estimation methods for walking model simulations - normal noise distribution

Noise from normal distribution											
		Cycle length, M									
FM	**Method**	**10**	**20**	**30**	**40**	**50**	**60**	**70**	**80**	**90**	**100**
0.3061	YW	551.2	541.8	451.4	443.7	346.1	148.3	61.0	51.1	41.7	26.9
0.3061	Burg	491.4	481.4	471.9	466.2	181.1	131.7	56.1	41.0	29.7	11.6
0.3061	VAAH	46.1	43.2	40.1	26.7	23.5	21.6	16.2	11.7	9.7	4.8
0.8436	YW	556.7	326.5	316.1	306.0	295.5	116.7	64.4	41.8	31.9	20.7
0.8436	Burg	436.0	426.2	419.6	221.7	218.2	126.4	121.5	119.8	56.5	16.6
0.8436	VAAH	38.7	26.5	24.2	21.7	18.1	11.7	6.5	4.1	3.1	1.9
		*** Values are multiplied by 10000 for more clarification**									

Table 8. The bias of different estimation methods for walking model simulations - uniform noise distribution

Noise from uniform distribution											
		Cycle length, M									
FM	**Method**	**10**	**20**	**30**	**40**	**50**	**60**	**70**	**80**	**90**	**100**
0.3061	YW	541.2	534.7	533.5	449.9	348.9	247.1	91.0	51.1	31.0	26.8
0.3061	Burg	531.4	523.5	526.8	443.4	343.1	231.6	81.2	43.7	26.2	11.4
0.3061	VAAH	48.8	41.1	42.1	24.7	25.5	19.6	18.4	9.2	6.3	2.2
0.8436	YW	436.1	426.5	326.7	221.9	223.1	222.0	212.2	177.5	16.2	6.5
0.8436	Burg	336.2	306.1	304.5	206.7	201.6	126.1	16.1	6.1	4.8	1.9
0.8436	VAAH	40.1	24.0	22.4	19.7	20.8	9.0	8.3	6.5	5.9	3.7
		*** Values are multiplied by 10000 for more clarification**									

Table 9. The bias of different estimation methods for walking model simulations - lognormal noise distribution

Noise from lognormal distribution											
		Cycle length, M									
FM	**Method**	**10**	**20**	**30**	**40**	**50**	**60**	**70**	**80**	**90**	**100**
0.3061	YW	551.1	446.0	343.7	243.8	146.9	91.6	51.4	41.2	36.1	21.0
0.3061	Burg	546.1	441.5	341.1	231.2	131.0	71.8	46.4	39.5	21.6	17.5
0.3061	VAAH	49.5	40.0	43.0	23.1	26.5	18.7	19.2	8.7	12.2	2.9
0.8436	YW	466.2	426.5	321.4	218.1	121.2	18.7	26.5	18.9	16.8	11.0
0.8436	Burg	446.4	418.9	316.9	211.5	106.6	103.8	98.2	97.1	24.4	8.9
0.8436	VAAH	41.5	23.0	27.8	18.9	19.4	8.6	7.3	4.4	2.3	1.8
		*** Values are multiplied by 10000 for more clarification**									

3.3 Conclusions

This chapter discussed the assessment techniques to measure the orbital stability of rhythmic executions. The conventional methods of Yule-Walker and Burg have been tested using simulations. The generated time series for different number of cycles have been used for each of the methods. The one-dimensional and multi-dimensional return maps with known Floquet multipliers have been evaluated. Simulation results for both Yule-Walker and Burg's method have shown the unaccepted bias in estimation of Floquet multipliers for both one-dimensional and multi-dimensional cases.

A new bias-reduction method has been proposed to measure the bias and reduce it from the estimation methods. The simulation results have shown the successful performance of the new algorithm for the generated time series for both one-dimensional and multi-dimensional cases. In order to evaluate the higher dimensional cases, the walking model of five-link biped robot has been used and the orbital stability of the model using VAAH's method has been measured.

The bias reduction method has been tested widely for different numbers of cycles and for different noise distributions, to assess the dependency of the method to noise distributions. The simulation results have shown the new method is completely independent of the noise distributions.

Chapter 4 - Results and Discussion

4.1 Discussion on bias-reduced methods

In this chapter different aspects of the methods are discussed and more comparisons of the results are analyzed. The one-dimensional case studied the bias reduction of a simple case of a return map. The results show Yule-Walker's and Burg's method has bias even after 50 or 60 stride numbers.

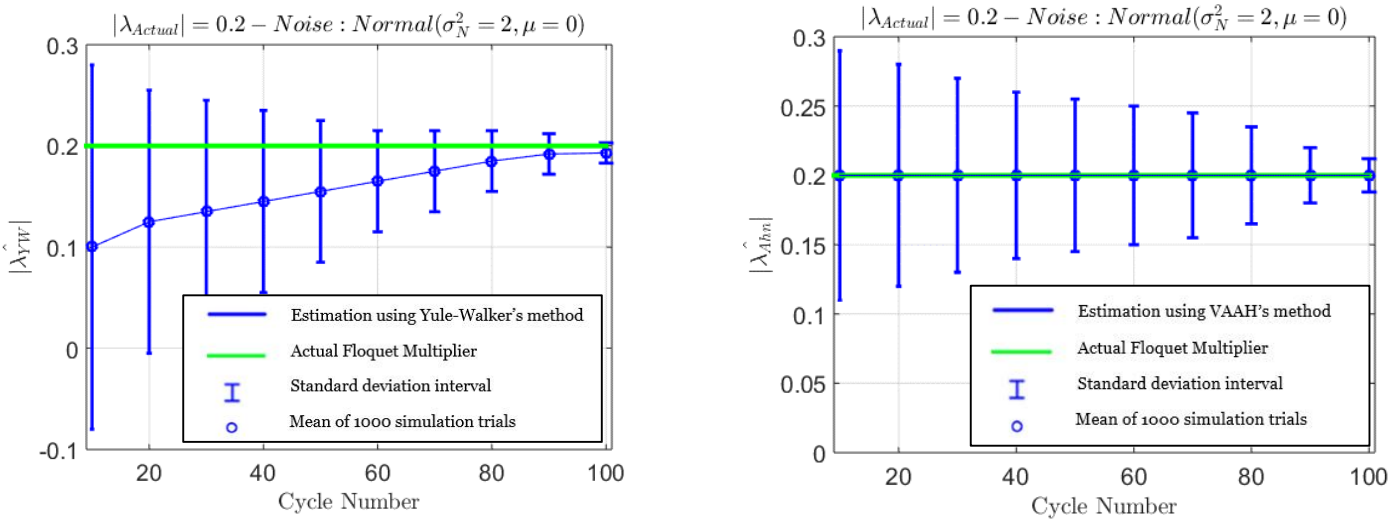

Figure 36. The comparison of Yule-Walker's method (left) and Ahn's method (right) with normal noise

As the figures show, the Yule-Walker's method starting from 10 cycles has mean of estimation far from the actual value. Even after 90 cycles, still the method could not converge to the actual value completely.

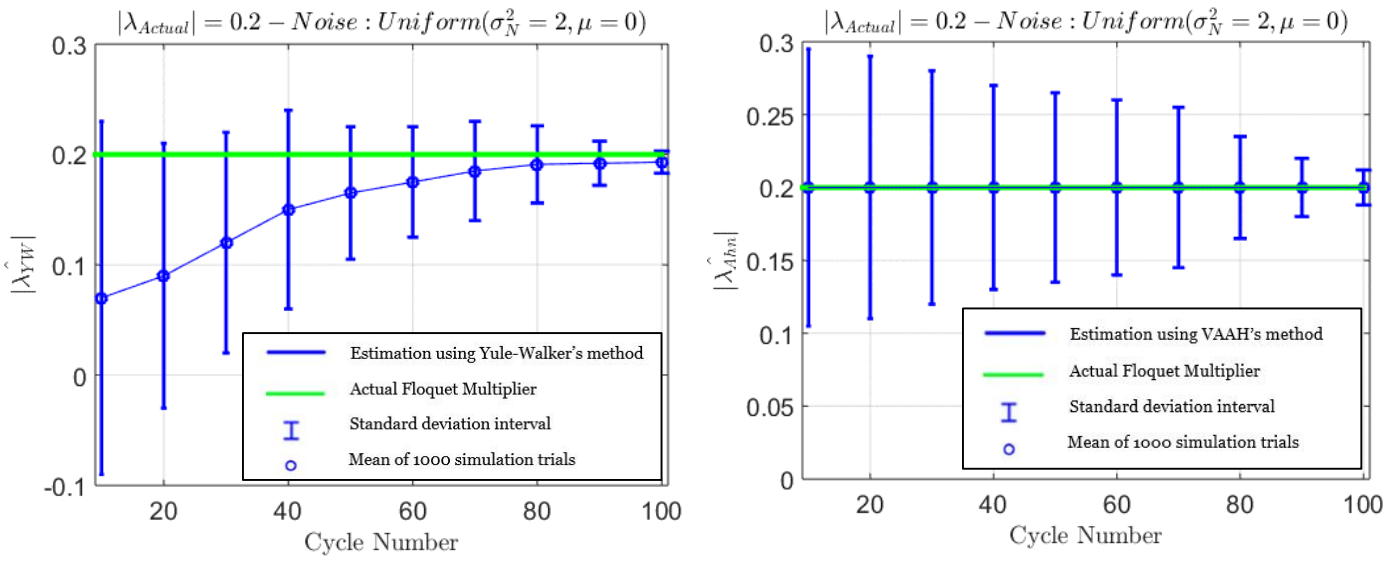

Figure 37. The comparison of Yule-Walker's method (left) and Ahn's method (right) with uniform noise

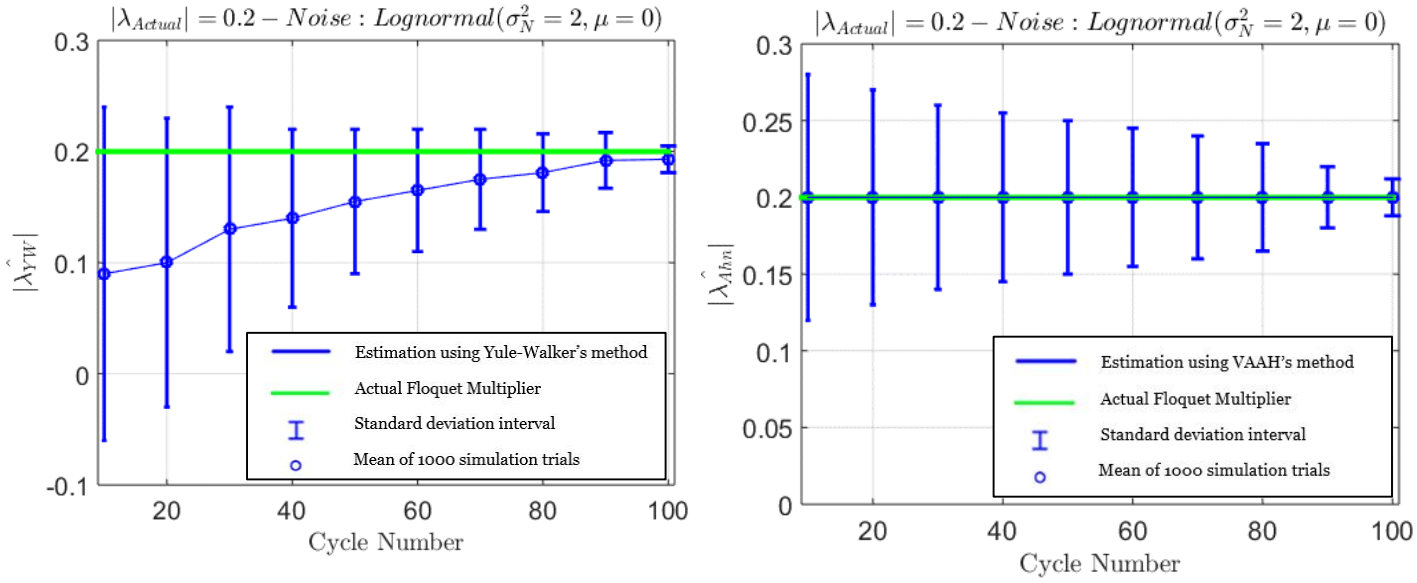

Figure 38. The comparison of Yule-Walker's method (left) and Ahn's method (right) with lognormal noise

Another difference is the independence of Ahn's method to different noise distributions. Also, as shown in Fig. 25, 26 and 27, the standard deviation estimated values using Ahn's method is less than Yule-Walker's method, which assures the accuracy of the method.

4.2 Dependency on Noise Level or distribution

The type of noise has been discussed in chapter 3, but the noise level needs to be changed to evaluate the methods in different noise levels for the variance or covariance. The simulation results have been repeated for both one-dimensional and multi-dimensional cases to show the dependency on the noise level in measuring of the Floquet multipliers. The variance σ_N^2 has been changed from values of two to four in covariance matrix of Ω_Δ as it is a diagonal matrix ofσ_N^2. The noise distribution kept constant as normal distribution. Also, for the sake of generality, the VAAH's method has been evaluated for walking model.

The results for Yule-Walker's method for walking model with higher noise level assure the bias. We conduct the VAAH's method for walking model for this situation and evaluated the results.

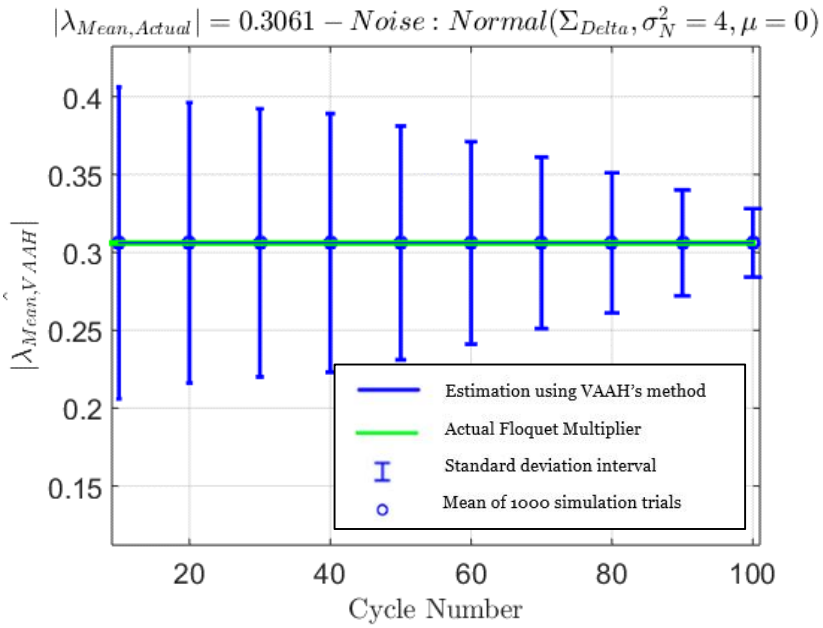

Figure 39. Walking model simulation, estimation of Floquet multipliers using VAAH's method – Mean of Floquet multipliers with normal noise and higher noise level

The mean values of the Floquet multipliers are estimated without bias for higher level of noises which assures the independency of the new method to noise level. The maximum value of the Floquet multiplier results are as the following for higher noise level:

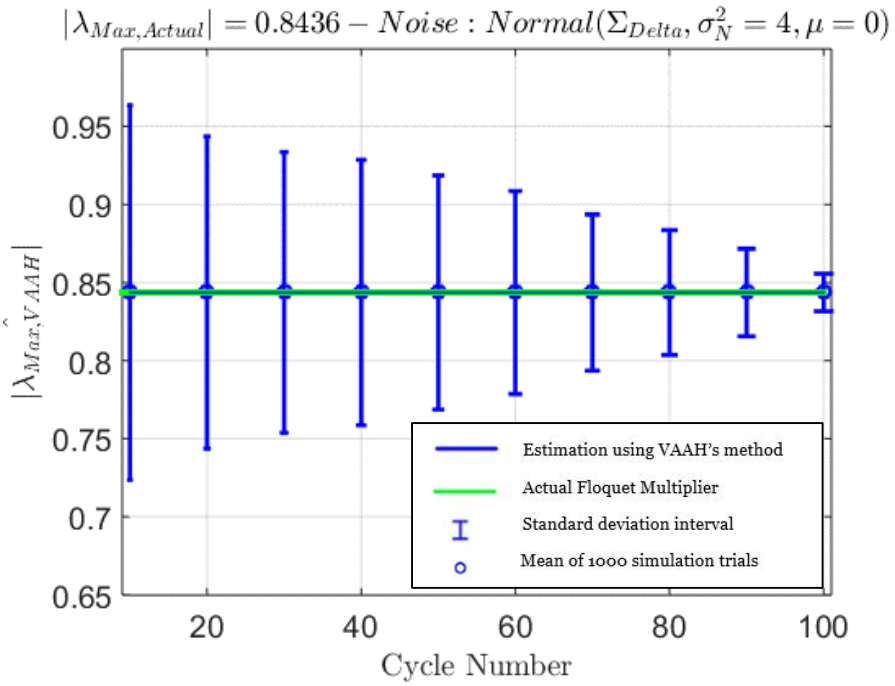

Figure 40. Walking model simulation, estimation of Floquet multipliers using VAAH's method – Maximum of Floquet multipliers with normal noise and higher noise level

The results for walking model with noise from normal distribution but higher noise level shows the independency of the VAAH's method to the noise level. This criterion has been evaluated by Ahn and Hogan for the one-dimensional case. They showed the one-dimensional bias reduction method has not had any dependency in case of higher noise levels [1].

4.3 Limitations

There have been a number of successful evaluations for the new proposed method. However, discussion of the possible limitations of this method is needed due to the wide range of applications and uncertainties.

As stated before, the new method assumed the noise added in each of the cycles has no correlation considering the neighbors' cycles. Application of this method to a system with anti-correlated or correlated noise has to be considered. Although, this assumption is widely accepted and supported in experimental tests especially human locomotion [30]. However, applying the VAAH's method to systems with correlated noise need a precaution to be considered for future studies.

The VAAH's method can significantly reduce the bias even with 10 cycles which most likely are the least number of cycles to conduct the experiments as the method relies on Yule-Walker's and Burg's methods to find the transformation matrix.

4.4 Conclusions

This chapter discussed the main challenges for each of the bias-reduced methods as well as noise level dependency of the new method. The simulation results have been repeated for the walking model to assess the orbital stability of the model in case of higher noise levels added to each cycle of walking execution with fixed noise distributions as normal type. The results have shown the successful independency of the new method to higher noise levels and assured the accurate measure of orbital stability even with more uncertainty included with the walking executions.

The possible limitations of the VAAH's method have been studies in case of assumptions related to the noise added to each cycle and number of cycles. The other assumption of having equal values of Floquet multipliers mentioned as essential future researches.

Chapter 5 - Conclusions

5.1 Main Contributions

There are different rhythmic processes in the nature and technology. Accurate measurement of the orbital stability is considered as an important challenge [1]. The main motivation of this research on the stability of rhythmic motions is for working with neurologically-impaired subjects' while they are walking. The level of their functional recovery needs to be monitored. However, they are usually incapable of walking for extended periods.

In the context of this thesis we analysed how to limit the window of the observations and increase the accuracy of the conventional stability measures. To this end, several simulation cases of rhythmic executions with known return maps for the limit cycle systems have been evaluated to assess these conventional methods. We then propose a new method that improves upon the previous methods' limitations and issues.

As discussed in the chapters, the existing methods of assessing the orbital stability have bias [7, 5]. The main contributions of the thesis are focused on conducting a straightforward methodology to reduce the bias of estimating the Floquet multipliers of the return map. This method would be applied for a limit cycle rhythmic motion to assess the orbital stability accurately. Also, reducing the number of required cycles to assess the orbital stability is necessary and important for working with impaired subjects to assess their locomotion performance improvements.

The studies of the orbital stability assessment for human locomotion evaluated the conventional methods to measure the index of orbital stability, Floquet multipliers such as Yule-Walker or Burg equations [28, 6, 32, 21]. In our research, we evaluated the conventional method and have determined that they have substantial bias [1]. The simplest case of assessing orbital stability in a one-dimensional case has been studied by Ahn and Hogan. They proposed a new bias-reduced method that quantified the amount of bias for the Floquet multiplier and then using the Yule-Walker's and Burg's estimations have found new bias-reduced value of Floquet multiplier [1].

Ahn and Hogan proposed a new method that substantially reduces the bias for the simplest case of a one-dimensional return map. However, one limitation of the proposed approach is that the new method is applicable to a one-dimensional case only. So, the main contribution of the thesis would be suggestion of a bias-reduced method applicable for multi-dimensional cases.

In this research, the extended version of the case for a multi-dimensional case has been proposed. We used basic linear algebra matrix decomposition to make the Jacobian matrix of the multi-dimensional return map as Jordan canonical blocks and then using the Ahn's method, we reduced the bias for each of the Floquet multipliers [1]. The main strengthens of the new method are robustness for different noise levels and distributions.

5.2 Recommendations

As an important application and future research would be assessment of the proposed method in real human walking kinematic data. We are now conducting more research on collecting the proper data to assess the orbital stability of human subjects. The initial cooperation with the research institutes at the hospitals have been conducted and results of this research will be discussed in the close future.

Whereas many stability indices have been proposed for clinical application [5, 7] , there is still no commonly accepted way to define or quantify locomotor stability. The main concern in the studies related to locomotors ability is to help clinicians in planning an adequate rehabilitation program to reach gait recovery. Applying the VAAH's method to the actual walking data could help in quantification of degree of motor stability during clinical tests. Also, monitoring this index could be preventing risk of fall during everyday activities.

As part of future research, analysis of bias reduction of direction of Floquet multipliers would be proper interest. Using bias reduction closed-form for eigenvectors could help to find the direction of each eigenvalue to assure the stability.

Bibliography

[1] J. Ahn and N. Hogan, "Improved assessment of orbital stability of rhythmic motion with noise," *PLoS ONE,* 2015.

[2] U. Saranli, M. Buehler and D. Koditschek, "A simple and highly mobile hexapod robot," *International Journal of Robotics Research,* pp. 616-31, 2001.

[3] A. KhazeniFard and F. Bahrami, "An energy efficient gait trajectory planning algorithm for a seven linked," in *International Conference of Electrical Engieering , IEEE*, Tehran, 2015.

[4] H. Miura and I. Shimoyama, "Dynamic walk of a biped," *The International Journal of Robotics Research,* pp. 60-74, 1984.

[5] J. Dingwell and H. Kang, "Differences between local and orbital dynamic stability during human walking," *Journal of Biomechanical Engineering.,* 2007.

[6] Y. Hurmuzlu and C. Basdogan, "Kinematics and dynamic stability of the locomotion of post-polio patients," *Journal of Biomechanical Engineering,* pp. 405-411, 1996.

[7] Y. Hurmuzlu and C. & Basdogan, "On the measurement of dynamic stability of human locomotion," *Journal of Biomechanical Engineering,* pp. 30-36, 1994.

[8] T. McGeer, "Dynamics and control of bipedal locomotion," *Journal of Theoretical Biology,* pp. 277-314, 1993.

[9] M. Coleman, "A stability study of a three-dimensional passive-dynamic model of

human gait," Cornell University, New York, USA, 1998.

[10] M. Garcia, A. Chatterjee, A. Ruina and M. Coleman, "Implest walking model: stability, complexity, and scaling," *Journal of Biomechanical Engineering,* pp. 281-288, 1998.

[11] A. Kuo, "Stabilization of lateral motion in passive dynamic walking," *International Journal of Robotics Research,* pp. 917-930, 1999.

[12] J. Morimoto and C. Atkeson, "Nonparametric representation of an approximated Poincaré map for learning biped," *Autonomous Robots,* pp. 131-144, 2009.

[13] F. Riva, M. Bisi and R. Stagni, "Gait variability and stability measures: minimum number of strides and within session reliability," *Computers in Biology and Medicine,* pp. 9-13, 2014.

[14] M. Coleman, A. Chatterjee and A. Ruina, "Motions of a rimless spoked wheel: a simple three-dimensional system with impacts," *Dynamics and Stability of Systems,* pp. 139-59, 1997.

[15] A. Goswami, B. Espiau and A. Keramane, "Limit cycles in a passive compass gait biped andpassivity-mimicking control laws," *Autonomous Robots,* p. 273–86, 1997.

[16] Y. Hurmuzlu, F. Génot and B. Brogliato, "Modeling, stability and control of biped robots—general framework," *Automatica,* p. 1647–64, 2004.

[17] P. McAndrew, J. Wilken and J. Dingwell, "Dynamic stability of human walking in visually and mechanically destabilizing environments," *Journal of Biomechanics,* p. 644–9, 2011.

[18] D. Hamacher, N. Singh, J. Van Dieën, M. Heller and W. Taylor, "Kinematic

measures for assessing gait stability in elderly individuals: a systematic review," *Journal of The Royal Society Interface,* pp. 1682-98, 2011.

[19] K. van Schooten, L. Sloot, S. Bruijn, H. Kingma, O. Meijer and M. Pijnappels, "Sensitivity of trunk variability and stability measures to balance impairments induced by galvanic vestibular stimulation during gait," *Gait & Posture,* pp. 656-60, 2011.

[20] A. Nayfeh and B. Balachandran, Applied nonlinear dynamics:analytical, computational, and experimental methods,, New York: Wiley, 1995.

[21] C. Klausmeier, "Floquet theory: a useful tool for understanding nonequilibrium dynamics," *Theoretical Ecology,* pp. 153-161, 2008.

[22] T. Engsted and T. Q. Pedersen, "Bias-correction in vector autoregressive models: A simulation study," *Econometrics ,* pp. 45-71, 2014.

[23] Yule GU., "On a method of investigating periodicities in disturbed series, with special reference to Wofer's sunspot numbers," *Philosophical Transactions of the Royal Society of London Series,* pp. 636-646, 1927.

[24] G. Walke, "On periodicity in series of related terms.," *Proceedings of the Royal Society of London Series,* pp. 518-32, 1931.

[25] B. JP, "Maximum entropy spectral analysis.," in *37th Annual International Meeting-Society of Exploration Geophysics*, 1967.

[26] M. De Hoon, T. Van der Hagen, H. Schoonewelle and H. Van Dam, "Why Yule-Walker should not be used for autoregressive modelling," *Annals of Nuclear Energy,* pp. 1219-1228, 1996.

[27] P. Broersen, "Finite-sample bias propagation in autoregressive estimation with the Yule-Walker method," *IEEE Transactions on Instrumentation and Measurement,* vol. 58, no. 5, pp. 1354-60, 2009.

[28] J. Dingwell and H. Kang, "Differences between local and orbital dynamic stability during human walking," *Journal of Biomechanical Engineering,* 2007.

[29] L. Smith, Jordan canonical form, Linear Algebra, New York: Springer, 1998.

[30] A. KhazeniFard, "Analysis and design a controller for control bipedal robot walking with cental pattern generator," School of ECE, University of Tehran, Tehran, Iran, 2015.

[31] A. Stocker and E. Simoncelli, "Noise characteristics and prior expectations in human visual speed perception," *Nature Neuroscience ,* pp. 578-585, 2006.

[32] Y. Hurmuzlu, C. Basdogan and S. D. , "Kinematics and dynamic stability of the locomotion of post-polio patients," *Journal of Biomechanical Engineering,* pp. 405-411, 1996.

Appendix 1 – Ahn and Hogan details of bias-reduction closed form

The closed-form bias reduction method for assessing the orbital stability proposed by Ahn and Hogan [1]. The following equations and derivations are from Ahn and Hogan research that has been used for VAAH method in extending the method to multi-dimensional cases.

Appendix S1

Bias of Floquet Multiplier Estimation by Linear Regression

The linear regression or least square fit estimates the Floquet multiplier as

$$\hat{\lambda} = \frac{\sum_{i=1}^{n-1}(x_i - \bar{x})(y_i - \bar{y})}{\sum_{i=1}^{n-1}(x_i - \bar{x})^2},$$

where $\bar{x}$ and $\bar{y}$ are the mean of $\{x_1, x_2, x_3, \ldots, x_{n-1}\}$ and $\{x_2, x_3, x_4, \ldots, x_n\}$ respectively, and $y_i = \lambda x_i + \delta_{i+1}$. The expectation of the bias becomes

$$E(\hat{\lambda} - \lambda) = E\left(\frac{\sum_{i=1}^{n-1}\left\{(x_i - \bar{x})(y_i - \bar{y}) - \lambda(x_i - \bar{x})^2\right\}}{\sum_{i=1}^{n-1}(x_i - \bar{x})^2}\right). \quad \text{(S1)}$$

Assuming a stable periodic process, or $|\lambda| < 1$, the AR process becomes stationary and thus has finite mean and variance, satisfying

$$E(x_{i+1}) = E(y_i) = E(x_i), \text{ and}$$
$$\text{var}(x_{i+1}) = \text{var}(y_i) = \text{var}(x_i).$$

The mean of x_i, or $\bar{x}$ is the solution of

$$E(x_{i+1}) = \lambda E(x_i) - E(\delta_{i+1}) = \lambda E(x_i) = E(x_i), \text{ which is zero.}$$

Therefore, re-writing the equation for the variance,

$$\sigma_x^2 = E(x_{i+1}^2) - E(x_{i+1})^2 = E(x_i^2) - E(x_i)^2, \text{ or}$$
$$\sigma_x^2 = E(x_{i+1}^2) = E((\lambda x_i + \delta_{i+1})^2) = \lambda^2 E(x_i^2) + 2\lambda E(x_i \delta_{i+1}) + E(\delta_{i+1}^2) = E(x_i^2).$$

By definition, x_i is a weighted sum of $\delta_1, \delta_2, \delta_3, \ldots, \delta_i$, none of which is correlated with δ_{i+1}. Therefore, $E(x_i \delta_{i+1})$ becomes zero. Then,

$$\sigma_x^2 = \lambda^2 E(x_i^2) + E(\delta_{i+1}^2) = \lambda^2 \sigma_x^2 + \sigma_\delta^2, \text{ or } \sigma_x^2 = \frac{\sigma_\delta^2}{1 - \lambda^2},$$

where σ_δ is the standard deviation of the noise, δ_k. Therefore, assuming a large enough number of cycles, the denominator of (S1) becomes

$$\sum_{i=1}^{n-1}(x_i - \bar{x})^2 = (n-1)\sigma_x^2 \cong \frac{(n-1)\sigma_\delta^2}{1 - \lambda^2}. \quad \text{(S2)}$$

Using (S1) and (S2), the expectation of bias can be approximated as

$$E(\hat{\lambda} - \lambda) \cong \frac{1 - \lambda^2}{(n-1)\sigma_\delta^2} E\left(\sum_{i=1}^{n-1}\left\{(x_i - \bar{x})(y_i - \bar{y}) - \lambda(x_i - \bar{x})^2\right\}\right). \quad \text{(S3)}$$

Using $y_i = \lambda x_i + \delta_{i+1}$,

$$\begin{aligned}
&\sum_{i=1}^{n-1}\left\{(x_i-\bar{x})(y_i-\bar{y})-\lambda(x_i-\bar{x})^2\right\}\\
&=\sum_{i=1}^{n-1}\left\{(x_i-\bar{x})(\lambda x_i+\delta_{i+1}-\bar{y})-\lambda({x_i}^2-2x_i\bar{x}+\bar{x}^2)\right\}\\
&=\sum_{i=1}^{n-1}\left\{x_i\delta_{i+1}-x_i\bar{y}+x_i\bar{x}\lambda-\bar{x}\delta_{i+1}+\overline{xy}-\lambda\bar{x}^2\right\}\\
&=\sum_{i=1}^{n-1}x_i\delta_{i+1}-(\bar{y}-\lambda\bar{x})\sum_{i=1}^{n-1}x_i-\bar{x}\sum_{i=1}^{n-1}\delta_{i+1}+(n-1)(\overline{xy}-\lambda\bar{x}^2).
\end{aligned} \tag{S4}$$

By definition of $\bar{x}$, the sum $\sum_{i=1}^{n-1}x_i$ can be re-written as $(n-1)\bar{x}$. Therefore, from (S4),

$$\begin{aligned}
&\sum_{i=1}^{n-1}\left\{(x_i-\bar{x})(y_i-\bar{y})-\lambda(x_i-\bar{x})^2\right\}\\
&=\sum_{i=1}^{n-1}x_i\delta_{i+1}-(n-1)(\overline{xy}-\lambda\bar{x}^2)-\bar{x}\sum_{i=1}^{n-1}\delta_{i+1}+(n-1)(\overline{xy}-\lambda\bar{x}^2)\\
&=\sum_{i=1}^{n-1}x_i\delta_{i+1}-\bar{x}\sum_{i=1}^{n-1}\delta_{i+1}.
\end{aligned} \tag{S5}$$

From (S3) and (S5),

$$E(\hat{\lambda}-\lambda)\cong\frac{1-\lambda^2}{(n-1){\sigma_\delta}^2}E\left(\sum_{i=1}^{n-1}x_i\delta_{i+1}-\bar{x}\sum_{i=1}^{n-1}\delta_{i+1}\right). \tag{S6}$$

By definition, $\hat{o}_p$ and $\hat{o}_q$ are independent when $p \neq q$. Therefore,

$$E(\hat{o}_p\,\hat{o}_q)=0 \text{ if } p\neq q \tag{S7}$$

because

$$\int_{-\infty}^{\infty}\int_{-\infty}^{\infty}\delta_p\delta_q f(\delta_p)f(\delta_q)d\delta_p d\delta_q=\int_{-\infty}^{\infty}\delta_q\left(\int_{-\infty}^{\infty}\delta_p f(\delta_p)d\delta_p\right)d\delta_q=0.$$

Note that the validity of (S7) does not depend on the specific shape of the distribution; the probability density function, f, can be any function as long as the mean of the noise is zero. Whether the distribution is symmetric like a normal and uniform distribution or asymmetric like a lognormal distribution, (S7) remains valid.

Now note that x_i is a weighted sum of $\hat{o}_1$, $\hat{o}_2$, $\hat{o}_3$, … $\hat{o}_i$, by definition in (1). Therefore, $E(x_i\hat{o}_{i+1})=0$ for each i, and $E\left(\sum_{i=1}^{n-1}x_i\delta_{i+1}\right)=0$. From (S6),

$$E(\hat{\lambda}-\lambda)\cong-\frac{1-\lambda^2}{(n-1){\sigma_\delta}^2}E\left(\bar{x}\sum_{i=1}^{n-1}\delta_{i+1}\right). \tag{S8}$$

By definition,

$$\begin{aligned} x_1 &= \delta_1 \\ x_2 &= \lambda\delta_1 + \delta_2 \\ x_3 &= \lambda^2\delta_1 + \lambda\delta_2 + \delta_3 \\ &\vdots \qquad\qquad \ddots \\ x_{n-1} &= \lambda^{n-2}\delta_1 + \lambda^{n-3}\delta_2 + \cdots + \delta_{n-1}. \end{aligned}$$

Therefore,

$$\begin{aligned} \bar{x} &= \frac{1}{(n-1)}(x_1 + x_2 + x_3 + \cdots + x_{n-1}) \\ &= \frac{1}{(n-1)}\left(\frac{1-\lambda^{n-1}}{1-\lambda}\delta_1 + \frac{1-\lambda^{n-2}}{1-\lambda}\delta_2 + \cdots + \frac{1-\lambda^2}{1-\lambda}\delta_{n-2} + \delta_{n-1}\right). \end{aligned} \tag{S9}$$

From (S8) and (S9),

$$E(\hat{\lambda}-\lambda) \cong -\frac{1-\lambda^2}{(n-1)^2\sigma_\delta{}^2} E\left(\left(\frac{1-\lambda^{n-1}}{1-\lambda}\delta_1 + \frac{1-\lambda^{n-2}}{1-\lambda}\delta_2 + \cdots + \delta_{n-1}\right)(\delta_2 + \delta_3 + \cdots + \delta_n)\right).$$

By (S7), any term with $\delta_p\,\delta_q$ $(p \neq q)$ does not contribute to the expectation, and only terms with $\delta_p{}^2$ remain. Therefore,

$$E(\hat{\lambda}-\lambda) \cong -\frac{1-\lambda^2}{(n-1)^2\sigma_\delta{}^2} E\left(\frac{1-\lambda^{n-2}}{1-\lambda}\delta_1{}^2 + \frac{1-\lambda^{n-3}}{1-\lambda}\delta_2{}^2 + \cdots + \delta_{n-1}{}^2\right). \tag{S10}$$

By definition, $E(\delta_p{}^2) = \sigma_\delta{}^2$, and (S10) becomes

$$\begin{aligned} E(\hat{\lambda}-\lambda) &\cong -\frac{1-\lambda^2}{(n-1)^2}\left(\frac{1-\lambda^{n-2}}{1-\lambda} + \frac{1-\lambda^{n-3}}{1-\lambda} + \cdots + \frac{1-\lambda^2}{1-\lambda} + 1\right) \\ &= -\frac{1-\lambda^2}{(n-1)^2}\left(\frac{(n-2) - (\lambda + \lambda^2 + \cdots + \lambda^{n-2})}{1-\lambda}\right) \\ &= -\frac{1-\lambda^2}{(n-1)^2}\left(\frac{(n-1) - (1 + \lambda + \lambda^2 + \cdots + \lambda^{n-2})}{1-\lambda}\right) \\ &= -\frac{1+\lambda}{(n-1)}\left(1 - \frac{1-\lambda^{n-1}}{(n-1)(1-\lambda)}\right). \end{aligned} \tag{S11}$$

Bias of Floquet Multiplier Estimation by the Yule-Walker Equation

The Yule-Walker equation estimates the Floquet multiplier as

$$\hat{\lambda}_{YW} = \frac{\sum_{i=1}^{n-1} x_i x_{i+1}}{\sum_{i=1}^{n-1} x_i^{\,2}}. \tag{S12}$$

Following the same procedure that derived above (S2), the variance of x_i, $\sigma_x^{\,2}$ becomes

$$\sigma_x^{\,2} = \frac{\sigma_\delta^{\,2}}{1-\lambda^2},$$

where σ_δ is the standard deviation of the noise, δ_k. Assuming a large enough number of cycles, the denominator of (S12) approximates

$$\sum_{i=1}^{n-1} x_i^{\,2} \cong \frac{(n-1)\sigma_\delta^{\,2}}{1-\lambda^2}. \tag{S13}$$

By definition of x_i, the numerator of (S12) becomes

$$\sum_{i=1}^{n-1} x_i x_{i+1} = \sum_{i=1}^{n-1} \left(\lambda^{i-1}\delta_1 + \lambda^{i-2}\delta_2 + \cdots + \delta_i\right)\left(\lambda^{i}\delta_1 + \lambda^{i-1}\delta_2 + \cdots + \delta_{i+1}\right). \tag{S14}$$

From (S13) and (S14),

$$E(\hat{\lambda}_{YW} - \lambda) \cong \frac{1-\lambda^2}{(n-1)\sigma_\delta^{\,2}} E\left(\sum_{i=1}^{n-1} \left(\lambda^{i-1}\delta_1 + \lambda^{i-2}\delta_2 + \cdots + \delta_i\right)\left(\lambda^{i}\delta_1 + \lambda^{i-1}\delta_2 + \cdots + \delta_{i+1}\right)\right) - \lambda$$

By (S7), any term with $\delta_p\,\delta_q$ $(p \neq q)$ does not contribute to the expectation, and only terms with $\delta_p^{\,2}$ remain. Therefore,

$$E(\hat{\lambda}_{YW} - \lambda) \cong \frac{1-\lambda^2}{(n-1)\sigma_\delta^{\,2}} E\left(\sum_{i=1}^{n-1} \left(\lambda^{2i-1}\delta_1^{\,2} + \lambda^{2i-3}\delta_2^{\,2} + \cdots + \lambda\delta_i^{\,2}\right)\right) - \lambda. \tag{S15}$$

Expanding what is inside Σ,

$$\begin{aligned}
&i=1: && \lambda\delta_1^{\,2}\\
&i=2: && \lambda^3\delta_1^{\,2} + \lambda\delta_2^{\,2}\\
&i=3: && \lambda^5\delta_1^{\,2} + \lambda^3\delta_2^{\,2} + \lambda\delta_3^{\,2}\\
&\vdots && \ddots\\
&i=n-1: && \lambda^{2n-3}\delta_1^{\,2} + \lambda^{2n-5}\delta_2^{\,2} + \cdots + \lambda\delta_{n-1}^{\,2}.
\end{aligned}$$

Calculating the sum,

$$\sum_{i=1}^{n-1}\left(\lambda^{2i-1}\delta_1^{\,2} + \lambda^{2i-3}\delta_2^{\,2} + \cdots + \lambda\delta_i^{\,2}\right) = \frac{\lambda-\lambda^{2n-1}}{1-\lambda^2}\delta_1^{\,2} + \frac{\lambda-\lambda^{2n-3}}{1-\lambda^2}\delta_2^{\,2} + \cdots + \frac{\lambda-\lambda^3}{1-\lambda^2}\delta_{n-1}^{\,2}.$$

Therefore, using $E(\delta_p^{\,2}) = \sigma_\delta^{\,2}$, (S15) becomes

$$E(\hat{\lambda}_{YW} - \lambda) \cong \frac{1-\lambda^2}{(n-1)\sigma_\delta^{\,2}}\left(\frac{(n-1)\lambda - (\lambda^{2n-1} + \lambda^{2n-3} + \cdots + \lambda^3)}{1-\lambda^2}\right)\sigma_\delta^{\,2} - \lambda, \text{ or}$$

$$E(\hat{\lambda}_{YW}) \cong \lambda - \frac{\lambda^3 - \lambda^{2n+1}}{(n-1)(1-\lambda^2)}. \tag{S16}$$

Appendix 2 – Dynamics of the motion of 5-link biped robot

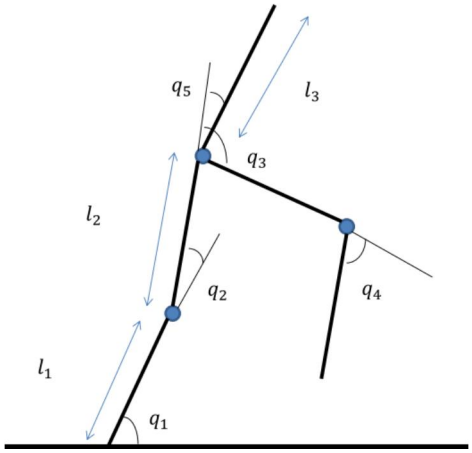

The single support phase dynamics:

$$M(q)\ddot{q} + CG(q,\dot{q}) = B(q)u \quad . \qquad (App.\,2.1)$$

If we write the model in state space form:

$$\begin{bmatrix} \dot{q} \\ M^{-1}(q)[-CG(q,\dot{q}) + B(q)u] \end{bmatrix} := f(x) + g(x)u \quad . \qquad (App.\,2.2)$$

Where $:= (q;\dot{q})$.

Also, the impact model would have:

$$x^+ = \Delta(x^-) \quad . \qquad (App.\,2.3)$$

Where $x^+ := (q^+;\dot{q^+})$ and $x^- := (q^-;\dot{q^-})$ is the state values just after and before impact respectively. For more details, see Khazenfard et. al. research [3, 30].